



TESIS DE DOCTORADO

DOCTORAL THESIS

**GEOMETRIC AND
HEMODYNAMIC ANALYSIS
OF THE RISK OF RUPTURE
OF INTRACRANIAL
ANEURYSMS**

JOSE LUIS THENIER VILLA

ESCUELA DE DOCTORADO

PROGRAMA DE DOCTORADO EN INVESTIGACIÓN CLÍNICA EN
MEDICINA

SANTIAGO DE COMPOSTELA

AÑO 2020





DECLARACIÓN DEL AUTOR DE LA TESIS
GEOMETRIC AND HEMODYNAMIC ANALYSIS OF THE RISK OF RUPTURE OF
INTRACRANIAL ANEURYSMS

D. José Luis Thenier Villa

Presento mi tesis, siguiendo el procedimiento adecuado al Reglamento, y declaro que:

- 1) La tesis abarca los resultados de la elaboración de mi trabajo.
- 2) En su caso, en la tesis se hace referencia a las colaboraciones que tuvo este trabajo.
- 3) La tesis es la versión definitiva presentada para su defensa y coincide con la versión enviada en formato electrónico.
- 4) Confirmo que la tesis no incurre en ningún tipo de plagio de otros autores ni de trabajos presentados por mí para la obtención de otros títulos.

En Santiago de Compostela, 11 de febrero de 2020

D. José Luis Thenier Villa





AUTORIZACIÓN DEL DIRECTOR/TUTOR DE LA TESIS

GEOMETRIC AND HEMODYNAMIC ANALYSIS OF THE RISK OF RUPTURE OF INTRACRANIAL ANEURYSMS

D. Miguel Gelabert González. Profesor titular de Cirugía del Departamento de Cirugía y Especialidades Médico-Quirúrgicas de la Universidad de Santiago de Compostela.

Dna. Rosa María Martínez Rolán. Profesora asociada del Departamento de Cirugía y Especialidades Médico-Quirúrgicas de la Universidad de Santiago de Compostela.

D. Antonio Riveiro Rodríguez. Profesor ayudante doctor del Departamento de Ingeniería de los Materiales, Mecánica Aplicada y Construcción de la Universidad de Vigo.

INFORMAN:

Que la presente tesis corresponde al trabajo realizado por D. José Luis Thenier Villa, bajo nuestra dirección y tutoría, y autorizamos su presentación, considerando que cumple con los requisitos exigidos por el Reglamento de Estudios Doctorales de la USC, y que no incurre en las causas de abstención establecidas en la Ley 40/2015.

De acuerdo con el artículo 41 del Reglamento de Estudios de Doctorado, declaran también que la presente tesis doctoral es idónea para ser defendida en base a la modalidad de COMPENDIO DE PUBLICACIONES, en los que la participación del doctorando fue decisiva para su elaboración.

La utilización de estos artículos en esta memoria, está en conocimiento de los coautores, tanto doctores como no doctores. Además, estos últimos tienen conocimiento de que ninguno de los trabajos aquí reunidos podrá ser presentado en ninguna otra tesis doctoral.

En Santiago de Compostela, 11 de febrero de 2020

Dr. Miguel Gelabert G.

Dra. Rosa María Martínez R.

Dr. Antonio Riveiro R.



De acuerdo con las directrices de la Escuela de Doctorado internacional (EDI) en ciencias de la salud de la Universidad de Santiago de Compostela (USC) (acuerdo de 3 de mayo de 2018), el doctorando José Luis Thenier Villa declara no tener ningún posible conflicto de intereses en relación con la presente tesis doctoral.

En Santiago de Compostela, a 11 de febrero de 2020





A mis mentores vivientes, a los eternos y a los etéreos...





AGRADECIMIENTOS

Este manuscrito no habría sido posible sin la colaboración de todo el personal del Hospital Álvaro Cunqueiro de Vigo, la Universidad de Vigo y la Universidad de Santiago de Compostela. Con el temor de omitir algún nombre debo agradecer por la colaboración incondicional a los doctores que conforman, o han conformado parte de dichos centros: Rosa Martínez, Antonio Riveiro, Miguel Gelabert, Eva Azevedo, Adolfo De La Lama, Pedro González, Lourdes Calero, Raúl Galarraga, Antía Domínguez, Pablo Sanromán, Álvaro Martín, Jesús González, Antonio Viladrich, María Regueira[†], Jorge Díaz, Cesáreo Conde.

Muchas otras personas se han visto involucradas en el largo proceso de la elaboración de esta tesis doctoral, destaco la enorme colaboración del Servicio de Neurocirugía del Hospital Universitario La Fe de Valencia a través de los doctores Pablo Miranda, Estela Plaza, Juan Antonio Simal, Tamara Cao, Laila Pérez, Amparo Roca, Ricardo Prat, Antonio Gutierrez, Inmaculada Galeano, Antonio Menéndez, José Pesudo, Carlos Botella, a quienes recuerdo con especial cariño.

Debo agradecer el apoyo que he recibido durante mi estancia en el extranjero como parte de este doctorado, gracias al Servicio de Neurocirugía del Hospital Universitario de Osaka, Japón por haber hecho que el choque cultural haya resultado inexistente a pesar del gran asombro que me inundó durante mi estancia en el país del sol naciente, recuerdo con especial cariño a los doctores: Koichi Hosomi, Satoru Oshino, Youichi Saitoh, Masayuki Hirata, Manabu Kinoshita, Hajime Nakamura, Takeo Nishida, Naoki Tani, Hui Ming Khoo y Haruhiko Kishima.

He tenido la fortuna de estar rodeado siempre de excelentes profesionales y personas; a pesar de la distancia, siempre he mantenido una relación estrecha con mi alma mater, la Universidad Autónoma Tomás Frías de Potosí, donde recibí enseñanzas que superan con demasía a la simple ciencia y me han valido para caminar con cierta holgura por la vida. Debo recordar con especial cariño a los doctores Holguer Chirveches, Antonio Barrios, Martha Espinoza, Adalid Mendoza, Filemón Veizaga, Rubén Albis, Alaín Marín, José Calle, Marlon Torres, Carlos Llave, Miguel Miranda, Mariela Berazaín, Gema Velazquez, Luis Montaña, Fredy Cayhuara, Daniel Salguero, Mayra Cari, Dante Andrade y Pamela Arriola, al tiempo que me disculpo de quienes haya obviado producto de mi mala memoria.

Debo agradecer al interminable soporte recibido por parte de mi familia durante todos estos años, a mis padres, Maritza Villa y Alberto Thenier, a mis hermanos María del Carmen Thenier y Walter Thenier, a mis abuelos Carmen Moreira y Walter Villa[†].

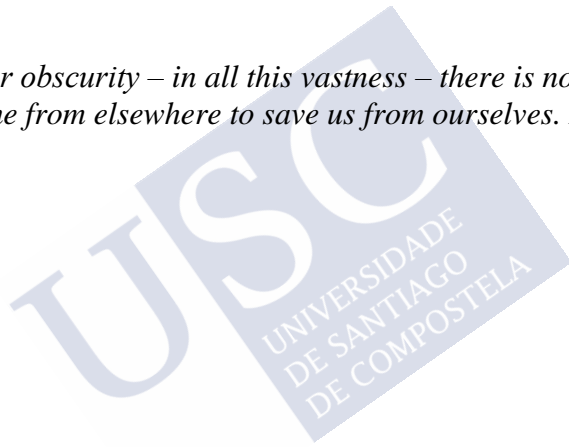
También existen personas que me han pedido expresamente no ser mencionadas, cumpliendo su petición, debo agradecer su infinito apoyo. Seguramente cuando lean estas líneas recordarán el momento en que me lo pidieron, por lo que destaco el carácter especial de este párrafo.

Agradezco también a nuestros pacientes y a sus familiares, a quienes aún a pesar de su sufrimiento han aceptado donar amablemente la información generada a lo largo de su enfermedad, colaborándonos muchas veces de maneras inesperadas, ayudándonos a explorar las entrañas de esta enfermedad tan devastadora.

Y finalmente un agradecimiento eterno a quienes nos encontramos y nos perdimos en el camino, fuimos fugaz resolana y jugamos nuestro rol en este ciclo, ... al ver ese granito de arena que dejamos en nuestras vidas solo me queda decir: “¡cuánto orgullo llevar un poquito de ti por esta vida!”.

“In our obscurity – in all this vastness – there is no hint that help will come from elsewhere to save us from ourselves. It is up to us.”

Carl Sagan





RESUMEN

Introducción y objetivos

Los aneurismas intracraneales son dilataciones de las paredes vasculares de las arterias cerebrales, su consecuencia más severa constituye la ruptura aneurismática causando hemorragia subaracnoidea y hematomas intracraneales, estas entidades conllevan una elevada mortalidad y se asocian a secuelas importantes entre los supervivientes, a pesar de ello, la mayoría de los aneurismas intracraneales no sangrarán a lo largo de la vida de un individuo. Cerca del 90% de los aneurismas intracraneales pertenecen al grupo de aneurismas saculares, los aneurismas fusiformes, traumáticos, fúngicos, disecantes y microaneurismas comprenden el 10% restantes.

Los aneurismas intracraneales están presentes en 3 a 8% de la población general, los factores principales que determinan su presencia son la enfermedad renal poliquística, la historia familiar de aneurismas intracraneales, la presencia de factores de riesgo modificables como el hábito tabáquico, el consumo de alcohol y la hipertensión arterial.

La historia natural de un aneurisma intracraneal se constituye de tres etapas, el desarrollo o génesis, el crecimiento o desestabilización y la ruptura aneurismática. Una debilidad innata o adquirida de la pared vascular arterial es un factor importante para el desarrollo de esta enfermedad. Los aneurismas intracraneales son más frecuentes en el género femenino y en el grupo de edades comprendido entre 35 y 60 años. En estudios epidemiológicos se ha vinculado su presencia con el hábito tabáquico, con un OR de 3.0, y con la hipertensión esencial con un OR de 2.9, la presencia de ambos resulta sinérgica con un OR de 8.3. La incidencia cruda en Europa es próxima a 6.3 casos por 100.000 personas-año. En ciertas localizaciones como Finlandia y Japón esta

incidencia es más elevada y alcanza a 16 y 28 casos por 100.000 personas-año respectivamente.

La hemodinámica de la circulación arterial cerebral juega un rol importante en la fisiopatología de esta enfermedad, la tensión de cizallamiento parietal es una de las variables hemodinámicas más estudiadas en aneurisma intracraneales, ésta se define como la fuerza por unidad de área producida por el estrés friccional de la viscosidad sanguínea actuando en paralelo a la pared arterial. Es una variable de medición compleja, por ejemplo, no existe una única tensión de cizallamiento parietal para un aneurisma dado, sino más bien es un valor que cambia en cada momento del ciclo cardíaco en cada región del aneurisma, para su estudio sistematizado se emplean frecuentemente promediados temporales y espaciales, de manera que se permita su comparación entre dos aneurismas de un mismo paciente y entre dos o más pacientes diferentes.

Los sitios de bifurcación arterial son puntos frecuentes para el desarrollo de aneurismas intracraneales, y se caracterizan por ser zonas con una tensión de cizallamiento parietal elevada y con un gradiente positivo a lo largo del flujo. El endotelio sensible a este insulto hemodinámico conduce cambios en su estructura a partir de señales bioquímicas que determinan la formación de sacos aneurismáticos. La geometría del aneurisma formado y la hemodinámica arterial son mutuamente causales, las paredes de un aneurisma precisan de un estrés hemodinámico determinado para mantener su estabilidad en un equilibrio de cambios eutróficos y destructivos. Las desviaciones hemodinámicas o geométricas de este punto de estabilidad conducen a cambios distróficos con la activación de señales bioquímicas que promueven la degradación de la matriz extracelular y la muerte celular. Este fenómeno puede alcanzar un punto en que la integridad estructural de la pared de un aneurisma se vea comprometida incluso con cambios leves de condiciones hemodinámicas como en condiciones fisiológicas, como es frecuente en la hemorragia subaracnoidea aneurismática. Una disciplina reciente denominada mecanobiología estudia las consecuencias biológicas y moleculares secundarias a cambios físicos, en este caso el entorno hemodinámico de la circulación cerebral.

Una hipótesis unificadora reciente propone que ciertos fenómenos fisiopatológicos están dirigidos por una tensión de cizallamiento baja y otros fenómenos están dirigidos por una tensión de cizallamiento anormalmente elevada, sin embargo, en gran parte de los estudios publicados a la fecha, incluyendo un meta-análisis reciente, se establece que la tensión de cizallamiento parietal reducida está vinculada a la ruptura aneurismática.

En esta serie de estudios se considera que una reducción de la tensión de cizallamiento parietal o un incremento del área de cizallamiento bajo (área del aneurisma sometido a una tensión de cizallamiento menor de 10% medida en la arteria eferente) son marcadores de un riesgo incrementado de ruptura aneurismática y se consideran como subsidiarios de un riesgo de ruptura teórico incrementado.

Dadas las limitaciones del estudio hemodinámico en un entorno real (por problemas éticos y metodológicos), grupos de investigación recientes se han volcado al estudio de la hemodinámica a partir de simulaciones por ordenador (in silico) empleando software ampliamente conocido y utilizado en el campo de construcción y aeronáutica. Los estudios de dinámica de fluidos computacional permiten el análisis del flujo en arterias cerebrales con una precisión más que aceptable con la ventaja de no modificar los resultados ni el riesgo procedimental de pacientes en un entorno real. Los estudios radiológicos almacenados en PACS o directorios locales de hospitales son una fuente valorable para realizar este tipo de estudios.

Esta serie se compone de tres estudios. En un entorno de esfuerzo computacional limitado, el presente trabajo fue optimizado para optimizarse en 3 problemas bien definidos y abordables por la metodología de dinámica de fluidos computacional. El objetivo del estudio 1 fue analizar el riesgo de ruptura de un aneurisma intracraneal distal después del tratamiento de un aneurisma proximal en casos de aneurismas intracraneales múltiples. El objetivo del estudio 2 fue determinar el riesgo de ruptura de aneurismas de arteria comunicante anterior en condiciones de asincronía y sincronía del flujo del segmento A1 de la arteria cerebral anterior. El objetivo del estudio 3 fue determinar el riesgo de resangrado después de la colocación de un

drenaje ventricular externo a través de métodos de dinámica de fluidos computacional a partir de estudios de imagen de pacientes reales apareados con un grupo de control.

Materiales y métodos

Durante el período de enero de 2008 hasta diciembre de 2017, 652 aneurismas intracraneales fueron diagnosticados en el Complejo Hospitalario Universitario de Vigo mediante angiografía por sustracción digital. En el estudio 1 se analizaron 24 pacientes con aneurismas intracraneales múltiples de un único árbol carotídeo. En el estudio 2 se analizaron 54 pacientes con aneurismas de arteria comunicante anterior, se excluyeron en este estudio pacientes con agenesias del segmento A1 de la arteria comunicante anterior y estudios subóptimos, los estudios de referencia en este estudio fueron la angiografía por resonancia magnética y angiografía por tomografía computarizada, la arteriografía al ser un estudio de lateralización selectiva fue descartada para este estudio. En el estudio 3 se consideraron 6 pacientes que sufrieron resangrado aneurismático después de la colocación de un drenaje ventricular externo y 6 sujetos de apareamiento (pacientes con características clínicas y radiológicas similares que no sufrieron resangrado después de la colocación de un drenaje ventricular externo).

El diseño de los estudios cumplió con los requisitos formales del Comité Ético de Investigación Clínica de Galicia siendo aprobado para su desarrollo con registro 2018/053.

Para esta serie de estudios se empleó la técnica de dinámica de fluidos computacional e interacción fluido-estructura, a partir de segmentaciones de sólidos derivados de estudios radiológicos fuente constituidos por la angiografía por sustracción digital (InSpace 3D, Siemens Medical Solutions, Forchheim, Alemania), angiografía por resonancia magnética y angiografía por tomografía computarizada.

Para la segmentación del aneurisma y sus arterias eferentes y aferentes se empleó el software Slicer 3D (Harvard Medical School, Boston, MA, USA) para MacOS, para el mallado de la segmentación se empleó el software Meshlab (Visual Computing Lab, Pisa, Italy) y para la

definición del sólido se empleó FreeCAD (Juergen Riegel, Werner Mayer, Yorik van Havre, OpenSource, <http://freecadweb.org/>), para la simulación de dinámica de fluidos computacional se empleó el software ANSYS Fluent en sus versiones 17.0 y 19.0 (ANSYS, ANSYS Inc., USA), la interacción fluido-estructura precisó el empleo del módulo Structural de ANSYS. Las mallas constaron de una resolución de alrededor de 100.000 elementos tetrahédricos y adicionalmente se estableció una capa viscosa de $0.1D$ (D =diámetro) adyacente a las paredes de los vasos sanguíneos para capturar los efectos frontera.

Los experimentos constaron de simulaciones transitorias, este tipo de simulación permite obtener análisis de momentos concretos del ciclo cardíaco a expensas de un coste computacional mayor comparado con estudios de estado estable. Se ha considerado a las paredes vasculares como estructuras rígidas en los estudios 1 y 2, y como estructuras elásticas en el estudio 3 de esta serie, ya que los cambios producidos por la introducción de un cambio de presión en las condiciones de contorno solo pueden ser capturados simulando paredes vasculares elásticas, en este aspecto el módulo elástico considerado fue de 5 MPa y la ratio de Poisson fue de 0.49, se consideró 0.4mm de grosor en la pared del aneurisma. En el estudio 3 se empleó el modelo de interacción fluido-estructura con simulaciones de dos vías, a partir del cual modificaciones geométricas condicionadas por el flujo sanguíneo son consideradas para siguientes iteraciones y las condiciones hemodinámicas son modificadas a partir de los mismos cambios geométricos hasta lograr la convergencia.

El flujo sanguíneo fue simulado considerando las características de un fluido no-newtoniano, es decir que la viscosidad es variable dependiendo de la tasa de cizallamiento a la que es sometida, los modelos no-newtonianos requieren esfuerzos computaciones mayores comparados con los modelos newtonianos pero ofrecen mayor fiabilidad ya que la sangre es por definición un fluido no newtoniano. En nuestra serie de estudios se empleó el modelo de Carreau-Yasuda, previamente descrito y empleado en estudios de reología sanguínea que involucran la vasculatura sistémica y cerebral.

Las condiciones de entrada correspondieron a una función sinusoidal con una velocidad pico de 0.5 m/s, una velocidad mínima de 0.1 m/s y una duración de 0.125 s en un periodo de 0.5 s en los tres estudios. Las condiciones de salida fueron determinadas como las correspondientes a la presión arterial media en las arterias cerebrales de primer orden (80 a 100mmHg). Para el estudio de interacción fluido-estructura se empleó una carga de presión a toda la geometría del aneurisma y de sus arterias circundantes, exceptuando las regiones de las salidas y entradas. La carga consistió en 5223 Pa en condiciones de presión intracraneal elevada y de 133 Pa en condición de presión intracraneal baja (simulando la descompresión de la presión intracraneal por un drenaje ventricular externo). Las medidas de resultado incluyeron la tensión de cizallamiento parietal promediada por el tiempo, la tensión de cizallamiento parietal máxima en pico de sístole, la tensión de cizallamiento parietal mínima a mitad de la diástole, la presión total promediada por el tiempo, el desplazamiento de la pared, la tensión de Von Mises y las áreas de alto y bajo cizallamiento.

Los estudios de geometría consideraron las mediciones de la altura del aneurisma, definido como la distancia máxima perpendicular entre el domo del aneurisma y el plano del cuello; la ratio de aspecto, definido como la relación entre la distancia máxima perpendicular y el diámetro medio del cuello del aneurisma. Otras variables como la distancia entre aneurismas se emplearon en el estudio 1 y otras como la angulación A1-A1, A1/A2 e índices de simetría se emplearon en el estudio 2.

Para el análisis estadístico se empleó el software SPSS versión 20 para MS Windows. El análisis inferencial se realizó a través de test no paramétricos para muestras dependientes en el caso de comparación pre y post tratamiento, y test para muestras independientes cuando se analizó aneurismas rotos y no rotos, el análisis multivariante se realizó con la técnica de regresión logística. Para el estudio 3, al tratarse de una muestra reducida, se empleó una metodología de apareamiento considerando controles con características similares de edad, género y localización del aneurisma. Se emplearon test no paramétricos para comparar grupos. Se asumió como significativo un valor p menor de

0.05. No se emplearon muestreos y se consideró a la población total en los grupos de estudio.

Resultados

El primer estudio se constituye de 24 casos de aneurismas intracraneales múltiples, se realizaron mediciones en el aneurisma distal antes y después del tratamiento de un aneurisma proximal. En 9 casos, dada la ausencia de estudios post-intervención se empleó la idealización del tratamiento del aneurisma en la fase de segmentación del aneurisma a través de la colocación de una intersección a nivel del cuello del aneurisma y de una regularización de la pared, el resultado fue validado por un neurocirujano o neurorradiólogo con experiencia.

El tamaño medio de aneurismas rotos fue de 7.05 mm y en aneurismas no rotos de 5.23 mm ($p=0.03$, test de Mann Whitney). El ratio de aspecto medio en aneurismas rotos fue de 2.04 y de aneurismas no rotos fue 1.22 ($p=0.02$, test de Mann Whitney). La tensión de cizallamiento parietal en mitad de diástole tuvo una media de 0.081 Pa en aneurismas no rotos y de 0.009 en aneurismas rotos ($p=0.04$, test de Mann Whitney). La tensión de cizallamiento parietal máxima en sístole tuvo una media de 49.67 Pa en aneurismas no rotos y de 86.88 Pa en aneurismas rotos ($p=0.04$, test de Mann Whitney).

El área de bajo cizallamiento pre-tratamiento tuvo una media de 54.15 y el área de bajo cizallamiento post-tratamiento de 56.93 ($p=0.02$, test de Mann Whitney).

La distancia interaneurismática media fue de 18.47 mm (rango de 6 a 31 mm). La diferencia pre y post-tratamiento del área de bajo cizallamiento mostró una correlación positiva débil con respecto a la distancia interaneurismática ($r=0.26$, $p=0.01$, correlación de Pearson).

El segundo estudio se constituye de 54 casos, se realizaron experimentos en condiciones de sincronía y asincronía (introduciendo 0.2s de retraso en la inyección de flujo en el segmento A1 de la arteria cerebral anterior no dominante). 45 casos (83.3%) se presentaron con aneurismas rotos y 9 casos como aneurismas no rotos o incidentales (16.7%).

La tensión de cizallamiento parietal promediada por el tiempo tuvo una media de 1.25 Pa en condiciones de asincronía y de 1.34 Pa en condiciones de sincronía ($p=0.05$, t de student para datos apareados), la presión media promediada por el tiempo tuvo una media de 13205 Pa en condiciones de asincronía y de 13495 Pa en condiciones de sincronía ($p=0.004$, t de student para datos apareados). La diferencia en el área de bajo cizallamiento tuvo un amplio rango de valores positivos a negativos (de -35.68 a 27.34), se agruparon los casos en área de bajo cizallamiento incrementada y área de bajo cizallamiento reducida en asincronía.

En el análisis multivariante por regresión logística, la presencia de un índice de simetría mayor y un ángulo A1-A2 dominante menor se relacionaron con un incremento en el área de bajo cizallamiento, con el subsecuente incremento del riesgo teórico de ruptura aneurismática en esta localización de aneurismas ($p=0.04$ y 0.04 respectivamente, regresión logística). El efecto de la asincronía en la presión intra-aneurismática promediada por el tiempo fue esencialmente negativa con una media de -289 Pa (rango de -4755.84 a 218.10 Pa).

En el tercer estudio 12 casos fueron analizados, 6 casos de resangrado después de la colocación de un drenaje ventricular externo y 6 controles de características similares que no presentaron resangrado.

El desplazamiento máximo de la pared en sístole tuvo una media de 0.34 mm en aneurismas que presentaron resangrado y de 0.36 mm en casos que no presentaron resangrado ($p=0.055$, test de Mann Whitney). La diferencia de desplazamiento parietal en condiciones de presión intracraneal elevada y reducida (HICP-LICP) fue calculada, el valor calculado fue de 0.01 mm en aneurismas que presentaron resangrado y 0.007 mm en aneurismas que no presentaron resangrado ($p=0.05$, test de Mann Whitney), esta diferencia es aún más significativa si solo se considera la zona de bajo cizallamiento (0.02 mm y 0.006 mm respectivamente) ($p=0.01$, test de Mann Whitney). La zona de máximo desplazamiento en aneurismas que presentaron resangrado era coincidente con el área de bajo cizallamiento, y en aneurismas que no resangraron el área de desplazamiento máximo era distante del área de bajo cizallamiento.

La tensión de Von Mises o estrés efectivo en condiciones de presión intracraneal elevada, tuvo una media de 4.77 MPa en aneurismas que presentaron resangrado y de 3.26 MPa en aneurismas que no presentaron resangrado ($p=0.25$, test de Mann Whitney). Bajo condiciones de presión intracraneal reducida, los aneurismas que presentaron resangrado presentaron una tensión media de 2.28 MPa y los aneurismas que no presentaron resangrado presentaron una tensión media de 1.42 MPa ($p=0.33$, test de Mann Whitney).

Conclusiones

Los cambios hemodinámicos en un aneurisma distal después del tratamiento de uno proximal determinan un perfil desfavorable incrementando el riesgo de sangrado o desestabilización del aneurisma distal en pacientes con aneurismas múltiples, estos hallazgos refuerzan el paradigma del tratamiento simultáneo, siempre que sea posible, de aneurismas intracraneales múltiples incluso si estos no están rotos.

Se estableció que la asincronía del flujo de los segmentos A1 de la arteria cerebral anterior ocasionan cambios hemodinámicos significativos en aneurismas de arteria comunicante anterior con un incremento del riesgo teórico de ruptura en casos de ausencia de asimetría de A1 y ángulos A1/A2 disminuidos, la sincronía del flujo es una variable que debería ser incluida en estudios posteriores que involucren esta zona de la circulación cerebral.

Se determinó que los cambios hemodinámicos después de la colocación de un drenaje ventricular externo incluyen un incremento del desplazamiento de la pared, que es más significativo a nivel de las áreas de bajo cizallamiento en aneurismas que presentaron resangrado. Esto sugiere que el resangrado se debe a una reapertura del aneurisma ya roto y no a una nueva ruptura del mismo aneurisma. Este riesgo es diferente del riesgo de sangrado de un aneurisma que nunca rompió y los resultados deben entenderse en ese contexto.

Las principales limitaciones del estudio incluyen la asunción de la teoría del cizallamiento parietal como desencadenante de la ruptura aneurismática como cierta, si bien la discusión sobre el rol de esta variable aún permanece en discusión abierta. La ausencia de perfiles de

velocidad personalizados para simular con mayor precisión el flujo sanguíneo cerebral, y los efectos del análisis radiológico en base a estudios cuando los aneurismas se encontraban ya rotos, al desconocerse la consecuencia geométrica del evento de ruptura. Estudios prospectivos podrían controlar mejor todas estas limitaciones.



ABSTRACT

Intracranial aneurysms are dilations of the arterial walls of the cerebral arteries, their most severe consequence is the aneurysmal rupture causing subarachnoid haemorrhage, an entity of high mortality and that is associated with important sequelae among survivors. The objective of this series of studies was to analyse the risk of rupture of multiple intracranial aneurysms, anterior communicating artery aneurysms and rebleeding after placement of an external ventricular drainage, using computational fluid dynamics methods from imaging studies of real patients. During the period from 2008 to 2017, 652 intracranial aneurysms were diagnosed in the University Hospital Complex of Vigo. Twenty-four patients with multiple intracranial aneurysms, 54 patients with anterior communicating artery aneurysms and 6 patients with their mating subjects who suffered bleeding after the placement of an external ventricular drainage were analysed. It was concluded that hemodynamic changes in a distal aneurysm after treatment of a proximal one determines an unfavourable profile, increasing the risk of bleeding or destabilization of the distal aneurysm in patients with multiple aneurysms; It was also established that the asynchrony of the flow of the A1 segments of the anterior cerebral artery causes significant hemodynamic changes in aneurysms of the anterior communicating artery with an increased theoretical risk of rupture in cases of absence of asymmetry of A1 and decreased A1/A2 angles; it was determined that hemodynamic changes after the placement of an external ventricular drainage include a significant increase in wall displacement at the level of low shear areas in aneurysms that presented bleeding.



RESUMO

Os aneurismas intracraniais son dilatacións das paredes arteriais das arterias cerebrais, a súa consecuencia máis severa constitúe a rotura aneurismática causando hemorraxia subaracnoidea, unha entidade de elevada mortalidade e que se asocia a secuelas importantes entre os sobreviventes. A finalidade desta serie de estudos foi analizar o risco de rotura de aneurismas intracraniais múltiples, aneurismas de arteria comunicante anterior e resangrado despois da colocación dun drenaxe ventricular externo a través de métodos de dinámica de fluidos computacional a partir de estudos de imaxe de pacientes reais. Durante o período de 2008 ata 2017, 652 aneurismas intracraniais foron diagnosticados no Complejo Hospitalario Universitario de Vigo. Analizáronse 24 pacientes con aneurismas intracraniais múltiples, 54 pacientes con aneurismas de arteria comunicante anterior e 6 pacientes cos seus suxeitos de apareamento que resangraron despois da colocación dun drenaxe ventricular externo. Concluíuse que os cambios hemodinámicos nun aneurisma distal despois do tratamento dun proximal, determina un perfil desfavorable incrementando o risco de sangrado ou desestabilización do aneurisma distal en pacientes con aneurismas múltiples; tamén se estableceu que a asincronía do fluxo dos segmentos A1 da arteria cerebral anterior ocasionan cambios hemodinámicos significativos en aneurismas de arteria comunicante anterior cun incremento do risco teórico de rotura en casos de ausencia de asimetría de A1 e ángulos A1/A2 diminuídos; determinouse que os cambios hemodinámicos despois da colocación dun drenaxe ventricular externo inclúen un incremento do desprazamento da parede máis significativo a nivel das áreas de baixo cizallamento en aneurismas que presentaron resangrado.



GLOSSARY OF ABBREVIATIONS

A1: First segment of the anterior cerebral artery

A2: Second segment of the anterior cerebral artery

ACA: Anterior cerebral artery

AcoA: Anterior communicating artery

CFD: Computational fluid dynamics

CT: Computed tomography

CTA: CT angiography

DSA: Digital subtraction angiography

FSI: Fluid-structure interaction

HiSA: High shear area

ICA: Internal carotid artery

ICH: Intracerebral hematoma

LSA: Low shear area

MCA: Middle cerebral artery

MRA: MRI angiography

MRI: Magnetic resonance imaging

OR: Odds ratio

QALY: Quality-adjusted life years

SAH: Subarachnoid hemorrhage

SD: Standard deviation

SDH: Subdural hematoma

TAWSS: Time-averaged Wall Shear Stress

WFNS: World Federation of Neurosurgical Societies

WSS: Wall shear stress



TABLE OF CONTENTS

1. Introduction	1
1.1. Risk factors for the formation of intracranial aneurysms...	2
1.2. Epidemiology and socioeconomic aspects of subarachnoid hemorrhage	3
1.3. Clinical aspects of subarachnoid hemorrhage	4
1.4. Natural history of intracranial aneurysms	6
1.5. Pathophysiology of cerebral aneurysms	8
1.6. Geometry of cerebral aneurysms	12
1.7. Computational fluid dynamics in intracranial aneurysms.	14
1.7.1. Source radiological studies	15
1.7.2. Boundary conditions in computational fluid dynamics.....	16
1.7.2.1. Temporal variation.....	16
1.7.2.2. Fluid.....	16
1.7.2.3. Wall features.....	17
1.7.2.4. Inlet and outlet conditions	18
2. Rationale and objectives	21
3. Subjects and methods.....	23
3.1. Population and sampling.....	23
3.2. Computational fluid dynamics	24
3.2.1. Geometry processing	24
3.2.2. Mesh processing.....	24
3.2.3. Fluid	26
3.2.4. Boundary conditions	26
3.2.5. Fluid-structure interaction	27
3.2.6. Experiments.....	27
3.3. Outcome variables.....	28
3.3.1. Wall shear stress.....	28

3.3.2.	Effective stress and Wall displacement.....	30
3.3.3.	Statistics.....	31
4.	Published studies.....	33
4.1.	Hemodynamic Changes in the Treatment of Multiple Intracranial Aneurysms: A Computational Fluid Dynamics Study.	33
4.2.	A1 asynchrony, a potential risk factor for the rupture of anterior communicating artery aneurysms: A computational fluid dynamics study.	33
4.3.	Effects of external ventricular drainage decompression of intracranial hypertension on rebleeding of brain aneurysms: A fluid structure interaction study	33
5.	Results	35
5.1.	Risk of rupture of multiple intracranial aneurysms after treatment of a proximal aneurysm	35
5.1.1.	Geometric and hemodynamic analysis of ruptured and unruptured aneurysms	37
5.2.	Effects of A1 asynchrony on the hemodynamics of anterior communicating artery aneurysms	41
5.2.1.	Geometric and hemodynamic characteristics	42
5.3.	Geometric and hemodynamic effects of intracranial pressure reduction by external ventricular drainage in the rebleeding phenomenon	47
5.3.1.	Wall displacement.....	47
5.3.2.	Von Mises stress.....	49
5.3.3.	Wall shear stress.....	49
6.	Discussion.....	51
6.1.	Multiple intracranial aneurysms: hemodynamic effect of the treatment of proximal intracranial aneurysms	51
6.2.	The asynchrony of A1 segment in the risk of rupture of anterior communicating artery aneurysms	53
6.3.	Effects of decompression of intracranial hypertension on rebleeding of cerebral aneurysms	55
6.4.	Limitations	58
7.	Conclusions	59
8.	Annexes	61

8.1. Favorable statement of the Clinical Research Ethics Committees of Galicia	63
8.2. Informed consent	65
9. References.....	71





1 INTRODUCTION

Cerebral aneurysms are abnormal dilations of the arterial wall of cerebral blood vessels, about 90% of them are saccular and about 85% of them are located in the anterior circulation of the Willis circle.¹ Its occurrence is more frequent in female with a ratio close to 3:2; 10 to 30% of the patients have multiple aneurysms.²

Cerebral aneurysms are most often found near the bifurcation points of intracranial vessels, where the presence of a high hemodynamic stress associated to an underlying structural abnormality, characterized by thinning or absence of tunica media and internal elastic lamina, leads to the formation of vascular dilations.³

Aneurysms are a heterogeneous group of vascular lesions, however 90% of them corresponds to the morphological group of saccular lesions, other types of aneurysms, such as fusiforms (sickle-shaped, affecting long segments of the arteries), traumatic, fungal (of infectious etiology), dissectants and microaneurysms represent the remaining 10% of the intracranial aneurysms.⁴

The highest prevalence of intracranial aneurysms is within the age range of 35 to 60 years, with a clear predominance of the female gender, although before the age of 40, the prevalence seems to be similar in both genders. The prevalence of unruptured intracranial aneurysms in the general population is estimated at around 2.8%, with some reports indicating that it could be as high as 8% in some populations.⁵

The presence of intracranial aneurysms is associated with smoking and essential hypertension with an odds ratio (OR) of 3.0 and 2.9 respectively; the simultaneous presence of both factors is synergistic, and is associated with an OR of 8.3 of occurrence of intracranial aneurysms.⁶

The main risk associated with intracranial aneurysms is their rupture. This causes intracranial hemorrhages, being the most frequent, subarachnoid hemorrhage (SAH), intracerebral hematomas (ICH) and subdural hematomas (SDH).

Subarachnoid hemorrhage is defined as the extravasation of hemorrhagic content into the subarachnoid space, between the pia mater and arachnoid membranes. There are multiple causes, including trauma, rupture of vascular malformations, neoplastic, venous and idiopathic.⁷

When there is a predominance of involvement of the subarachnoid spaces of the basal cisterns or the Sylvian fissure and the clinical presentation is not associated with a recent significant trauma, the most frequent cause of subarachnoid hemorrhage is the spontaneous rupture of an intracranial aneurysm.⁷

In this text, unless otherwise specified, the term subarachnoid hemorrhage will only refer to this nosological entity, defined as the hemorrhagic stroke secondary to the rupture of an intracranial aneurysm.

1.1 RISK FACTORS FOR THE FORMATION OF INTRACRANIAL ANEURYSMS

The evolutionary process of an intracranial aneurysm is dynamic. The study of formation of aneurysms de novo and aneurysms induced by hemodynamic stress in animals and in isolated human cases suggest that the formation of the intracranial aneurysm is an initial and well-defined event.⁸ The formation of an intracranial aneurysm requires the presence of an intrinsic weakness of the vascular wall with a genetic or acquired substrate. More recently, prominent phenomena of inflammation, degeneration and tissue repair mediated by hemodynamic stress has been described in the pathophysiology of cerebral aneurysms.^{8,9}

The prevalence of incidental aneurysms in first-degree relatives of patients diagnosed with intracranial aneurysms is higher than that reported in the general population, with an estimated prevalence of 4 to 9%. These aneurysms tend to rupture at younger ages and with smaller sizes compared with the rest of the population.¹⁰⁻¹²

Certain genetic and medical conditions have been directly associated with intracranial aneurysms in population studies; these include: Ehlers-Danlos syndrome, fibromuscular dysplasia, hereditary haemorrhagic telangiectasia, arteriovenous malformations, Klinefelter syndrome, Marfan disease, microcephalic osteodysplastic primordial dwarfism, neurofibromatosis, Noonan syndrome, pheochromocytoma, polycystic kidney disease, pseudoxanthoma elasticum, tuberous sclerosis, alpha-1 antitrypsin and alpha-glucosidase deficiency, among others.⁴

1.2 EPIDEMIOLOGY AND SOCIOECONOMIC ASPECTS OF SUBARACNOID HEMORRHAGE

Subarachnoid hemorrhage (SAH) due to rupture of an intracranial aneurysm accounts for 5 to 10% of all stroke cases.^{13,14} The crude incidence of SAH is estimated in 9 cases per 100,000 person-years, but this is variable and depends on the geographical location, age and gender of the study population.^{13,15}

In Europe, the crude incidence rate of SAH is estimated at 6.3 cases per 100,000 person-years in 2010; in a temporal trend analysis, a reduction in its incidence at a rate of 1.7% per year was identified.¹⁶

The incidence in other geographical regions is significantly higher. In Finland, it reaches 16.6 cases per 100,000 person-years and in Japan, 28 cases per 100,000 person-years.¹⁶⁻¹⁸

In epidemiological and treatment studies, the incidence is significantly higher in women, the overall specific incidence in the female gender is 11.5 per 100,000 person-years and it is 9.3 per 100,000 person-years for the male gender. Studies including independent populations as a risk factor also show greater incidence of subarachnoid hemorrhage in

female.¹⁶ The estimated female : male ratio is between 1.24 and 1.74.^{13,19}

Half of the patients suffering from subarachnoid hemorrhage are under 55 years old,¹⁵ and up to a third of them are under 50,²⁰ most survivors of the haemorrhagic event will have some degree of residual cognitive impairment and long-term disability.^{15,21,22} This entity is associated with a loss of productive life years of equal magnitude to the ischemic stroke.^{15,23}

Subarachnoid hemorrhage is related to a loss of 11.1 years of life expectancy and 10.4 years of quality-adjusted life (QALY) compared to the general population.²⁴ Even in patients with a favourable functional outcome, some problems such as the sensation of loss of energy and certain emotional disorders such as anxiety and depression are frequent in the evolution of these patients.²⁵⁻²⁷

1.3 CLINICAL ASPECTS OF SUBARACNOID HEMORRHAGE

The clinical presentation of intracranial aneurysms is very heterogeneous. The ISUIA study (International Study of Unruptured Intracranial Aneurysms),²⁸ found that the diagnosis of an unruptured aneurysm was established under the following circumstances: in the evaluation of another intracranial aneurysm (30%), headache (23%) ischemic stroke or transient ischemic attack (10% each), cranial nerve palsy (8%), seizures (3%), and other less frequent.

The most important complication of an intracranial aneurysm is subarachnoid haemorrhage. Most cases of aneurysm rupture occur spontaneously and without a clear trigger, although some factors such as defecation, intense exercise, sexual activity, or altered emotional states have been described as triggers of bleeding.⁹

The most common clinical presentation of the rupture of an intracranial aneurysm is an extremely intense headache accompanied or preceded by a deterioration of the level of consciousness towards a

coma. In a 10 to 43% of patients, a previous episode of headache called “sentinel headache” has been described in the weeks or days previous to the haemorrhagic debut.²⁹

The most reliable and generalized diagnostic method in clinical practice is brain computed tomography (CT), which offers a 98-100% of sensitivity if performed in the first 12 hours, and 93% in the first 24 hours, with a detriment of its performance over time.³⁰

In most of the centres, once the diagnosis is established by a simple CT scan, a CT angiography sequence is performed at the same time. The sensitivity to detect 7 mm or larger aneurysms is 95% with this technique, although it is reduced to 53% for aneurysms of 2 mm or less.³¹ For this reason, the definitive study for the diagnosis and therapeutic planning of an intracranial aneurysm is digital subtraction arteriography (DSA), given its excellent temporal and spatial resolution.

One of the most potent predictors of the functional outcome of aneurysmal subarachnoid hemorrhage is the clinical severity of the disease, defined according to the initial neurological examination immediately after the acute event or in the emergency admission. In recent decades, clinical grading systems have been developed with the intention of predicting the neurological and vital prognosis of patients.

Several scales have been described in the literature, from the historic Bortell scale published in 1956,³² continuing with one of the most used scales, the Hunt and Hess scale, described in 1986,³³ to the World Federation of Neurosurgical Societies scale (WFNS), described in 1988,³⁴ which has managed to homogenize the classification of the clinical presentation in many studies published as to date.

Despite their wide use in clinical practice and medical research, the previously described scales are imprecise in statistical terms. The margins of each additional point on a given scale are not always related to worse prognoses.

A study assessing the Hunt and Hess scale found statistically significant differences only between grades 2 and 3 and between grades 3 and 4 regarding the prognosis of the patients studied.³⁵ Another independent study showed that there is no significant difference between grades 0 through grade 2 of this same scale.³⁶

The WFNS scale, another ordinal (nonlinear) scale, has similar limitations, grades 2 to 3, and grades 3 to 4 have less defined prognostic limits.³⁵

It is likely that this over-fractionation error could be reduced if more differentiated segmentations are used, such as classifying them as high-grade (HH 4 and 5) and low-grade subarachnoid hemorrhage (HH 1-3). Despite these limitations, the clinical grading at the time of admission is considered the single most important prognostic factor in this disease.³⁷

1.4 NATURAL HISTORY OF INTRACRANIAL ANEURYSMS

Intracranial aneurysms are present in 3 to 8% of the general population.^{2,9,38} Despite this, most intracranial aneurysms will never rupture during the normal life span of an individual.^{39,40} The main conditions or risk factors that have an effect on the natural history of an unruptured intracranial aneurysm include polycystic kidney disease, family history, modifiable risk factors such as smoking, alcohol consumption and high blood pressure.^{41,42} The OR of aneurysmal rupture in a smoking and hypertensive patient reaches up to 15, a value that almost doubles the OR of the occurrence of aneurysms in the presence of the same risk factors independently.⁴³

Two large studies regarding the natural history of cerebral aneurysms support most current guidelines for the management of non-ruptured aneurysms. The ISUIA (The International Study of Unruptured Intracranial Aneurysms) is a prospective study conducted in 1692 patients with aneurysms larger than 2 mm, including 1077 patients without previous haemorrhagic events. The two variables associated with an increased risk of rupture of an intracranial aneurysm in this

study were the location and size of the aneurysm; other less relevant factors were also identified in this study.²⁸

The second study was UCAS (Unruptured Cerebral Aneurysms), and it was conducted in Japan. In this study, which included patients with aneurysms larger than 3 mm, 5720 patients were included. In a similar way to the previous study, the size of the aneurysm, its shape, and its location were the variables directly associated with the risk of rupture of the intracranial aneurysm.⁴⁴

A more recent study, based on a systematic review and using a pooled analysis in 8382 patients from 6 prospective studies, proposed a practical scoring system called PHASES, with the intention of predicting the risk of rupture of an aneurysm at 5 years. The variables included in this study were population (assigning a higher risk to Finnish and Japanese individuals), arterial hypertension, age over 70 years, aneurysm size greater than or equal to 20 mm, previous subarachnoid hemorrhage, and location of the aneurysm in a circulation other than the middle cerebral artery and internal carotid artery.⁴⁵

The management of intracranial aneurysms makes it necessary to compare the risks of the natural history of the disease in the absence of any intervention and the risks derived from surgical or endovascular procedures that are intended to reduce or eliminate the risk of bleeding from an aneurysm.

In a certain group of patients, watchful waiting (with control of modifiable risk factors and monitoring by non-invasive imaging methods) would be the best option, for example, when dealing with patients older than 60 years with aneurysms smaller than 7 mm without family history or previous bleeding events.⁴⁶ On the other hand, in patients younger than 60 years, with aneurysms greater than 7 mm and with risky location or morphology, a personalized treatment plan should be considered, considering a surgical or endovascular intervention, according to the experience of the center, characteristics of the patient and aneurysm to be treated.⁴⁰

There is no consensus regarding the modality, timing and duration of follow-up in patients with unruptured aneurysms. In most medical centres, non-invasive methods such as computed tomography angiography or magnetic resonance angiography are selected, reserving digital subtraction angiography for cases where a pre-treatment reassessment is necessary.⁴⁷⁻⁴⁹

A follow-up every 6 to 12 months initially and annual or bi-annual controls later may be a valid strategy in most cases. In young patients or patients with known risk factors, non-invasive follow-up may extend throughout the life of the individual.⁴

1.5 PATHOPHYSIOLOGY OF CEREBRAL ANEURYSMS

The natural history of an intracranial aneurysm is generally divided into 3 phases, formation or genesis, growth or destabilization and rupture as the final event.

The factors that mediate the formation, growth and rupture of intracranial aneurysms are not fully understood, there is an open discussion about the stages of the natural history of the disease and the different pathological phases of this entity.

It is known through experimental studies in animals and analytical studies in humans that there are inflammatory and hemodynamic factors that govern this sequence of events. For example, specific studies have shown an increase in the degradation of the extracellular matrix mediated by matrix metalloproteinases (MMPs) and smooth muscle cell apoptosis, which progressively generate a weakness of the arterial wall, resulting in progressive growth and participating in the event of aneurysm rupture.^{50,51}

The interaction of hemodynamic and inflammatory phenomena is the object of study of mechanobiology, a relatively recent scientific field that explores the complex interactions between the flow and the molecular cascades responsible for maintaining vascular structures that are subjected to hemodynamic stress.

Table 1 shows the main mediating pathways and inflammatory molecules involved in the formation, growth and rupture of intracranial aneurysms.

Table 1. Inflammatory and mediating pathways involved in the formation and rupture of intracranial aneurysms

Pathway	Mediators
Endothelial dysfunction	IL-1 β , NF- κ B, Ets-1, MCP-1, Reactive oxygen species, Nitric oxide (NO), endothelial NO synthase, inducible NO synthase, Angiotensin II, Phosphodiesterase-4, Prostaglandin E2, E selectin, P selectin, vascular cell adhesion protein 1 (VCAM1), intercellular adhesion molecule 1 (ICAM1)
Phenotypic modulation and loss of SMCs	TNF- α , KLF-4, IL-1 β , P47phox, MCP-1, MMPs, Adhesion molecules
Macrophages, M1/M2 imbalance, leukocyte infiltration	MCP-1, NF- κ B, Ets-1, MMPs, IL-1 β , TNF- α , Normal T cell expressed and secreted, Monokine induced by γ -interferon, Interferon- γ -induced protein-10, Eotaxin, IL-8, IL-17
Vascular remodeling, cell death	MMP and cathepsins, TNF α , IL-1 β , IL-6, Toll-like receptor 4, Fas, NO, Complement, IgG, IgM, Basic fibroblast growth factor, transforming growth factor α and β , and vascular endothelial growth factor, Reactive oxygen species
IL-1 β indicates interleukin 1 β ; KLF-4, Kruppel-like transcription factor 4; MCP-1, monocyte chemoattractant protein-1; MMP, matrix metalloproteinase; NF- κ B, nuclear factor- κ B; SMC, smooth muscle cell; and TNF α , tumor necrosis factor- α .	

(From *Review of Cerebral Aneurysm Formation, Growth, and Rupture* by Nohra Chalouhi et al. Free access license in *Stroke*)

The formation of an intracranial aneurysm is directly related to the resistance of the arterial wall and the hemodynamic forces. The cerebral arterial wall is especially prone to hemodynamic stress due to the absence of an external elastic lamina, medial elastin, supporting adventitia and absence of dense perivascular tissues. On the other hand, the irregular distribution of its ramifications and vascular

tortuosities secondary to atherosclerosis favour the development of aneurysms in these segments.⁵²⁻⁵⁵

The existence of an acquired or inherited wall weakness lowers the threshold of the pathological response, triggering pathological events more easily, in a greater extent or in a shorter interval of time.^{2,37,56}

Animal studies have demonstrated the important role of hemodynamics in the pathophysiology of intracranial aneurysm formation.⁵¹ Arterial bifurcation sites are subjected to hemodynamic forces characterized by an increase in the wall shear stress (WSS, force per unit area produced induced by frictional stresses due to the blood viscosity and acting parallel to the artery wall) and a positive WSS gradient along the flow.⁵⁷

The endothelium exerts biological responses modifying its structure through cascades of biochemical signals that would be responsible for the formation of the aneurysm, the earliest signs of this phenomena would be the loss of the local internal elastic lamina, thinning of the tunica media and formation of “lumps”.⁵⁸⁻⁶⁰ Subsequent events involve remodeling, degradation and cell death.⁶¹

Aneurysm growth is the result of an imbalance between eutrophic changes (cell proliferation and extracellular matrix production) and destructive changes (cell death and extracellular matrix degradation) in the aneurysm wall.

Hemodynamic phenomena play an important role in this process, it is thought that aberrant hemodynamics through abnormal wall shear stress leads to destructive biological changes of the aneurysmal wall that overcome the eutrophic changes that maintain the integrity of the aneurysm, so that the aneurysm wall becomes weak and prone to rupture.^{3,62}

Intracranial aneurysm rupture has been associated with intense physical activity or high blood pressure states, such as emotional stress.⁶³ However, most aneurysms suffer a rupture under conditions of routine activities for a normal individual, clearly demonstrating a substrate of intrinsic wall weakness to the point that any minimal

physical effort could generate tensile forces that exceed the ultimate strength of the aneurysmal wall causing the rupture of the aneurysm.

The gradient of the vascular wall is therefore an important factor in the phenomenon of rupture of the intracranial aneurysm.^{3,64}

Recently a unifying hypothesis was proposed. According to this hypothesis, some aberrant mechanobiological phenomena are directed by high wall shear stresses while other phenomena are driven by low wall shear stresses. This is an example of the complexity of the pathophysiology of intracranial aneurysms.

The vascular responses mediated by the two stress conditions are summarized in Table 2.³

Table 2. Vascular responses to aberrant wall shear stress reported in the literature

Pathobiologic Responses to High WSS and Positive WSS Gradient	Pathobiologic Responses to Low WSS and High OSI
Endothelial cell damage	Proinflammatory ECs that are “leaky” and “sticky”
Endothelial cell turnover	Increased reactive species of oxygen
MMP production by mural cells	Increased inflammatory cell infiltration
ECM degradation	MMP production by macrophages
Medial thinning	SMC proliferation and migration
Mural cell apoptosis	Thrombus formation

(From: *HighWSS or LowWSS? Complex Interactions of Hemodynamics with Intracranial Aneurysm Initiation, Growth, and Rupture: Toward a Unifying Hypothesis* by Meng et al. Free access license in *American Journal of Neuroradiology*)⁶⁵

1.6 GEOMETRY OF CEREBRAL ANEURYSMS

The geometry of the aneurysms refers to the static measurements of the dimensions of an aneurysm and its parts, its afferent artery, its efferent branches and the different angles and ratios that these components offer when they are related to each other.

These measurements can be achieved through studies of digital subtraction angiography, considered the gold standard for the diagnosis of intracranial aneurysms,⁶⁶ and also from by computed tomography angiography (CTA) or magnetic resonance angiography (MRA); these last two methods being accessible in most hospitals in developed countries.

Regarding CTA, its acquisition is rapid in an urgent scenario, it has excellent sensitivity and its resolution is adequate to perform multiplanar and volumetric reconstructions of enough quality for the evaluation of the morphology of intracranial aneurysms in most of the cases.⁶⁷

Although the large prospective studies cited above analyse only the maximum dimension of the aneurysm as a geometric variable, other geometric aspects are also important.

The geometric measurements of intracranial aneurysms can be done in a 2-dimensional and 3-dimensional fashion. The most commonly used ones are described below:

- Size: It is defined as the maximum perpendicular distance between the aneurysm dome and the aneurysm neck plane.⁶⁸
- Aspect Ratio (AR): Defined as the ratio between the maximum perpendicular height and the average diameter of the aneurysm neck.⁶⁹ A commonly used value for a threshold is 1.6, studies suggest that a value above this threshold is associated with a significantly higher risk of rupture.^{70,71}
- Aneurysm-vessel size ratio (AVR): Defined as the ratio between the maximum height of the aneurysm and the average diameter of the main artery.⁷² Several studies have identified

this variable as strongly associated with aneurysmal rupture.
72-74

- Bottleneck factor (BF): Defined as the ratio between the maximum aneurysm width and the aneurysm neck diameter.
75
- Undulation Index (UI): Defined as $IO = 1 - (V/V_{ch})$, where V is the volume of the aneurysm above the plane of the neck, and V_{ch} is the volume of a convex shell on the same geometry. An aneurysm without concavities will have an IO of 0.⁶⁸
- Non sphericity index (NSI): Similar to the previous one, it uses the surface area of the aneurysm with respect to the aneurysm volume and its deviation from a perfect hemisphere is found, it is obtained as follows: $INE = 1 - (18\pi)^{1/3} V^{2/3}/S$, where S is the surface, and V corresponds to the total aneurysm volume.⁶⁸
- Vessel angle (VA): Defined as the angle formed between the centerline of the vessel and the plane of the aneurysm neck.⁷⁶
- Angle of inclination of the aneurysm (AIA): Defined as the angle formed between a line joining the centroid of the neck with the most distant point of the dome of the aneurysm and the line of the plane of the neck.⁷²

Table 3 summarizes the areas under the curve for rupture (ruptured/unruptured) with respect to geometric variables of intracranial aneurysms in various studies.

Table 3: Geometric variables and area under the curve in the evaluation of the rupture status of intracranial aneurysms

	Dhar et al, 2008 ⁷²	Raghavan et al, 2005 ⁶⁸	Xiang et al, 2011 ⁷⁷
Size	0.58	0.60	0.62
AR	0.70	0.72	0.63
AVS	0.83	-	-
UI	0.75	0.80	0.72
NSI	0.75	0.83	0.73
VA	0.85	-	-
AIA	0.54	-	-

1.7 COMPUTATIONAL FLUID DYNAMICS IN CEREBRAL ANEURYSMS

Every phenomenon in nature is transient by definition; it is variable in the course of time. Therefore, an aneurysm cannot be understood as a single geometric entity insensitive to changes over time.

The blood flow that passes through a cerebral artery exerts mechanical forces and entails geometric changes in the arterial wall that unquestionably participate in the pathophysiology of cerebral aneurysms.

During the last decades, the development of more advanced and higher resolution imaging techniques has been accompanied by hardware and software development in computer technology. The convergence of both disciplines has allowed studies where the paradigm of computational fluid dynamics (CFD), widely used in fluid mechanics, were applied. This allowed the transfer of this discipline to the field of medical research through *in silico* studies,⁷⁸ with the additional advantage that no real patient is subjected to procedural risks, allowing the study of cerebral hemodynamics with a more than acceptable precision.

1.7.1 Source radiological studies

The most frequently used techniques in clinical practice are CTA, MRA and DSA. This last one is considered the gold standard for diagnosis and management of intracranial aneurysms, given their great spatial and temporal resolution.

CTA consists of an acquisition of computed tomography in which an iodinated contrast medium is used to increase the density of the content of the cerebral arteries in order to highlight them with respect to other tissues. This study has the advantage of being widely accessible in most healthcare centres and is performed quickly in an urgent environment, making it the ideal test in the initial evaluation of subarachnoid hemorrhage. Its spatial resolution ranges from 0.23 mm to 0.7 mm depending on the acquisition machine.⁶⁵ A common dataset includes between 400 and 1000 images allowing to perform three important post-processing techniques that were used in this study: multiplanar reconstruction (MPR), maximum intensity projection (MIP) and volume rendering.⁷⁹

MRA consists of a magnetic resonance acquisition in which gadolinium-based contrast media or speed discriminators (time-of-flight) are used to highlight the cerebral arteries from the rest of the tissues. The spatial resolution of this test ranges between 0.6 mm and 1.2 mm according to the technique and the acquisition machine.⁸⁰ This acquisition also allows multi-plan reconstructions, maximum intensity projections and volume rendering.

Digital subtraction arteriography has been used for decades for the diagnosis and treatment of intracranial aneurysms. It is undoubtedly the study with the highest spatial resolution, with a real resolution of 0.15 mm for 3D-DSA studies.⁸¹

Post-processing is done in dedicated stations. In our center, we employ Inspace 3D software (InSpace 3D™, Siemens Medical Solutions, Forchheim, Germany) for generating complex datasets of up to 400-1000 images. In this modality of study the computation time is considerably extended given the large spatial resolution of the data.

1.7.2 Boundary conditions in computational fluid dynamics

1.7.2.1 Temporal variation

Computational fluid dynamics studies use mathematical models to simulate blood flow conditions. There are many mathematical models and formulas that can be assumed for experiments. The simulation can be adjusted with less or greater rigor to the biological reality depending on the assumptions that are established.

First, the simulations can be transient or steady state. The transient simulations have the advantage of capturing the temporal variability, in our case, the pulsatility of the blood flow, and let us obtain results of any moment of the cardiac cycle; however, the computational cost is significantly greater as the mathematical model must be solved for each time step.

By contrast, steady-state simulations require lower computational cost by providing similar results when compared to time-averaged results from transient simulations,⁸² becoming an efficient alternative when the objectives are consistent with this method.

Transient simulations were always used in our studies, since the determination of maximum and minimum values in systole and diastole can only be obtained in this way.

1.7.2.2 Fluid

The blood flow can be simulated considering the conditions of the fluid as Newtonian or Non-Newtonian. Blood behaves like a non-Newtonian fluid, i.e. its viscosity changes depending on the shear rate to which it is subjected. Non-Newtonian models in simulations require more computational effort compared to Newtonian models.

The power law model, Casson model and Carreau-Yasuda model are the most commonly used non-Newtonian models.⁸³

In our studies, the dynamic viscosity of the blood was modelled using the Carreau-Yasuda model. This model takes the form of:

$$\frac{\mu - \mu_{\infty}}{\mu_0 - \mu_{\infty}} = \left(1 + (\Gamma\dot{\gamma})\right)^{\frac{n-1}{2}}$$

where μ is the effective viscosity dependent on the shear rate $\dot{\gamma}$, μ_0 is the zero-shear viscosity ($\mu_0 = 0.056 \text{ Pa}\cdot\text{s}$), μ_{∞} is the infinite shear viscosity ($\mu_{\infty} = 0.0035 \text{ Pa}\cdot\text{s}$), Γ is the time constant ($\Gamma = 3,313 \text{ s}$) and n is the power law index ($n = 0.3568$).

1.7.2.3 Wall features

The wall of the artery under study can be simulated as a rigid or elastic material. In nature, the blood vessel walls are viscoelastic materials (i.e. energy transmitted into them is both stored and dissipated due to the elastic and viscous properties of arterial walls). Their composition based on collagen and elastin determine the grade of elasticity,⁸⁴ and the main variability in vivo is granted by atherosclerosis, decreasing its effective elasticity.⁸⁵

Similar to previous observations, the addition of elastic characteristics to arterial walls in computational fluid dynamics simulations significantly increases the computational cost as the geometry and boundary conditions can change during the simulation, and a fluid-structure interaction (FSI) problem must be solved. However, according to some studies, the influence on the wall shear stress is insignificant.⁸⁶ This is consistent with a decrease in the peak value and of the temporal and spatial averaging values of the wall shear stress.⁸⁷

If the objective of the study is only the analysis of the blood flow through a computational fluid module, rigid wall studies could be considered acceptable. However, studies incorporating the elastic properties of vessel walls can provide more information about the real

wall shear stress and the degree of wall displacement,⁸⁸ which are both important variables when assessing the phenomenon of rupture of an intracranial aneurysm.

In our studies, on the analysis of multiple aneurysms and the asynchrony of A1 segment of the anterior communicating artery aneurysms, only the ANSYS Fluent software (V19.0, ANSYS Inc., USA) was used. We assumed the vessel walls as rigid structures, considering that the efficiency of this method does not affect the results obtained. This is considered in accordance with the objectives of the studies.

On the other hand, in the study of decompression of intracranial hypertension, when a second space (intracranial space) comes into play, we consider important to perform a two-way fluid-structure interaction simulation. In this case, the fluid simulation will produce structural changes in the arterial wall, which are consolidated in the structural (mechanical) simulation and moved into the next iteration to the fluid simulation, and producing changes in it. Assuming elastic arteries is fundamental in this approach.

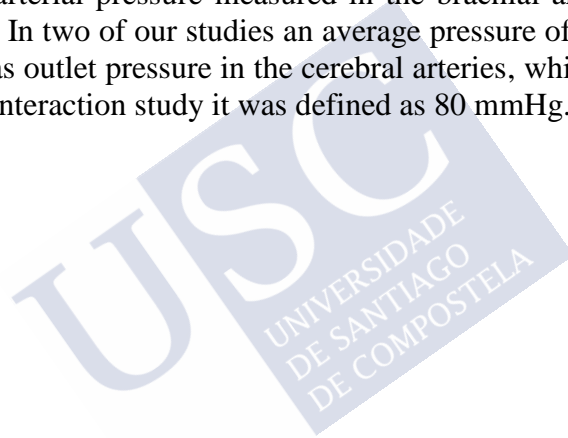
1.7.2.4 Inlet and outlet conditions

Computational fluid dynamics studies must assume initial conditions in their simulation from which hemodynamic changes will occur and will generate the results. Pressure conditions at the inlets and outlets of arterial vessels are important because they significantly alter hemodynamic characteristics.

For the inlet conditions, certain functions (sinusoidal, parabolic, Womersley, etc.) can be used to take into account the pulsatile nature of blood flow. We could use as inlet condition data obtained from the pulse of individual patients to simulate real conditions with a greater reliability. However, the authors who have compared both kind of approaches observed that the difference in results obtained when considering the velocity profile changes are less important as compared to changes in geometry. In the same way, in retrospective studies in which the specific characteristics of the

patients' pulse are absent, the use of common assumptions in the inlet velocity profile seems acceptable.⁸⁹

The outlet function of the blood vessels is mainly subordinated to the blood pressure in the vessel under study. In a normal individual, the average blood pressure is inversely proportional to the calibre and branching of the artery of study. In the cerebral arteries of the Willis circle (anterior cerebral artery, middle cerebral artery, anterior communicating artery, posterior cerebral artery) an average pressure of 80-100 mmHg is assumed as an outlet pressure; in the internal carotid artery the pressure is similar to the systemic arterial pressure measured in the brachial artery (100-120 mmHg).⁹⁰ In two of our studies an average pressure of 100 mmHg is assumed as outlet pressure in the cerebral arteries, while in the fluid-structure interaction study it was defined as 80 mmHg.





2. RATIONALE AND OBJECTIVES

Intracranial hemorrhage due to the rupture of a cerebral aneurysm is a frequent cause of mortality and morbidity worldwide. Studies of hemodynamics of cerebral arteries are unfeasible in a real environment and cannot be performed for ethical reasons; because of that, many research groups have turned their efforts to studies based on computational fluid dynamics during the last decade, using computer simulations based on radiological studies obtained from real patients. This methodology offers the advantage that it does not alter the clinical results of patients in their actual environment and allows patients to be evaluated both retrospectively and prospectively.

Source radiological studies, usually remain stored in hospital computer databases (PACS), and are extremely valuable for conducting analytical and retrospective studies evaluating the geometry of aneurysms and any of their derivatives. It also allows the possibility of application in computational fluid dynamics and fluid-structure interaction studies, and to collect many epidemiological and clinical data that otherwise could not be contrasted with the results of these computational techniques.

In the period from January 2008 to December 2017, 652 intracranial aneurysms were diagnosed in the University Hospital Complex of Vigo by digital subtraction angiography. Other studies, such as CTA, MRA or DSA was present in almost all of them.

Being a very extensive dataset, in a scenario of limited computational effort, the objectives of the present work were optimized in 3 aspects.

- To determine the geometric and hemodynamic characteristics of multiple intracranial aneurysms undergoing treatment: by means of which a group of patients with multiple intracranial aneurysms of the same vascular tree were obtained from the database and computational fluid dynamics experiments were conducted.
- To determine the hemodynamic effects of asynchrony of the A1 pulse on the risk of rupture of anterior communicating artery aneurysms: in this study, population was segmented by the presence of anterior communicating artery aneurysms and computational fluids dynamics experiments were performed.
- To determine the geometric and hemodynamic effects of the decompression of intracranial hypertension by an external ventricular drainage in the rebleeding of cerebral aneurysms: patients who presented a rebleeding phenomenon were segmented and two experiments were conducted under different conditions using fluid interaction structure (FSI).

3. SUBJECTS AND METHODS

3.1 POPULATION AND SAMPLING

In the period from January 2008 to December 2017, 652 cases of intracranial aneurysms were diagnosed through digital subtraction arteriography in the University Hospital Complex of Vigo.

Of the total of patients, 106 patients (16.25%) had multiple intracranial aneurysms and 23 patients had multiple aneurysms of the same vascular tree meeting the inclusion criteria for the study 1. Sampling was not performed and all the patients were included.

For the second phase of the study, 122 patients (18.71%) with aneurysms of the anterior communicating artery met the inclusion criteria for the study 2. Patients with agenesis of segment A1 of the anterior communicating artery and patients with suboptimal studies were excluded. The final study population were 54 patients. Sampling was not performed all the patients who met criteria were included.

For the study of fluid-structure interaction, patients with radiological studies dated from the period between 2014 and 2017 were considered, since many radiological studies did not offer sufficient quality for analysis; In this period, 219 intracranial aneurysms were diagnosed, 6 of these cases presented rebleeding after the placement of a EVD, meeting the inclusion criteria for the study 3. Sampling was not performed and the total number of patients who fulfilled these criteria was included.

The design met all formal research ethics requirements and was approved by the Research Ethics Committee of Galicia with registration number 2018/053.

3.2 COMPUTATIONAL FLUID DYNAMICS

3.2.1 Geometry processing

In the first study, full carotid trees, from their emergence from the cavernous sinus to their terminal branches immediately distal to the aneurysm of the most distal location, were selected. Source studies included digital subtraction arteriography, computed tomography angiography and magnetic resonance angiography. The used source radiological study varied according to the objective of the study and the quality of the source images.

For the second study, the anterior communicating artery complex was established as geometry, consisting of the first segment of the anterior cerebral artery (A1) on both sides, and at least 3 mm of the second segment of the anterior cerebral artery (A2) of both sides of the cerebral circulation. The reference studies were computed tomography angiography and magnetic resonance angiography, excluding digital subtraction arteriography as it is a selective study that does not allow the single segmentation of two independent circulations, being necessary the use of registration techniques for that purpose complicating the methodological process and also the analysis of the results.

For the third study, the aneurysm under study and at least 5 mm of its efferent artery and 5 mm of its arterial branches were selected. The reference study in this study was digital subtraction angiography.

3.2.2 Mesh processing

The segmentation and generation of an STL (stereolithography) file was carried out using the software Slicer 3D (Harvard Medical School, Boston, MA, USA) for MacOS.⁹¹ The surfaces were processed using the free access software Meshlab (Visual Computing

Lab, Pisa, Italy) and FreeCAD (Juergen Riegel, Werner Mayer, Yorik van Havre, OpenSource, <http://freecadweb.org/>) in order to create meshes with a density of around 100,000 tetrahedral elements for a subsequent treatment at ANSYS software (ANSYS v19.0, ANSYS Inc., USA). In addition, a layer of $0.1D$ (D = diameter of the vascular lumen) was added adjacent to the vessel walls to capture the effects of the boundary layer. The segmentation and meshing steps from the source images are illustrated in Figures 1 and 2.

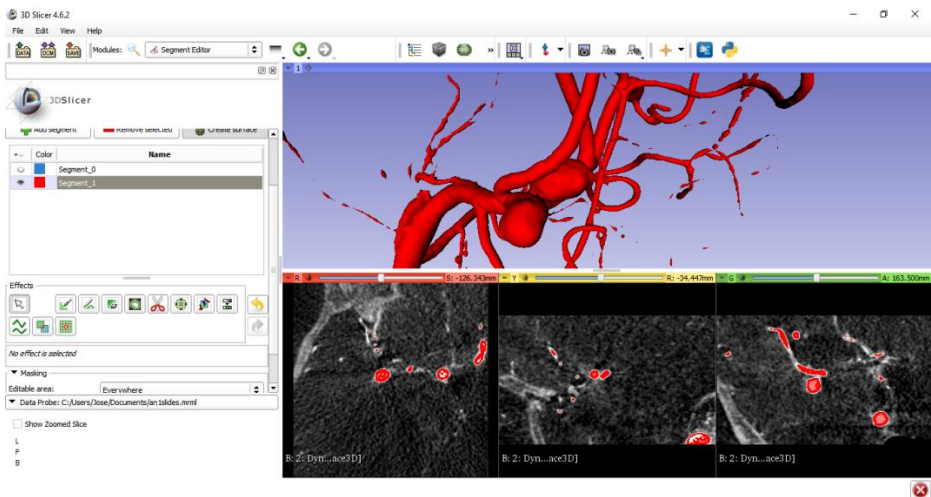


Figure 1. Semiautomatic threshold segmentation in an InSpace3D Siemens study, this is a case of multiple aneurysms of the middle cerebral artery.

In the third study, where the blood vessel walls are assumed to be an elastic solid, a solid model was used. The artery wall is assumed as a linearly elastic, isotropic, incompressible and homogeneous material, with a density of $\rho_a=1000\text{kg/m}^3$. The elastic modulus and the Poisson ratio were assumed to have a value of $E=5$ MPa and $\nu=0.49$ respectively. The thickness of the aneurysm wall was considered as $t=0.4$ mm.⁹²

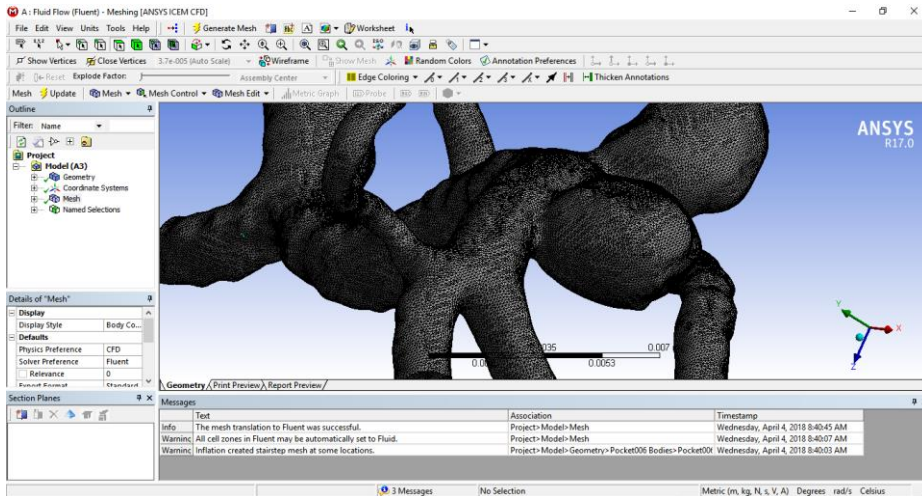


Figure 2. Meshing of a case of multiple aneurysms of the middle cerebral artery, GUI: ANSYS 17.0. Previously processing: Meshlab.

3.2.3 Fluid

The ANSYS Fluent 17.0 (first study) and 19.0 (second and third studies) software was used to solve the Navier-Stokes and mass conservation equations, under the assumption of laminar, incompressible and non-Newtonian flow.

The governing equations are described below:

$$\rho(\vec{u} \cdot \nabla \vec{u} + \nabla p - \mu \Delta \vec{u} = 0)$$

$$\nabla \cdot \vec{u} = 0$$

The dynamic viscosity of the blood was modelled using the Carreau model, described above.

3.2.4 Boundary conditions

Transitional pulsatile simulations averaged over several cardiac cycles were performed. Regarding inlet conditions, a sinusoidal profile with a peak velocity of 0.5m/s and a minimum velocity of 0.1m/s was simulated. The pulse duration was 0.125s, and the period of 0.5s. The outlet conditions were determined by pressures close to

the mean arterial pressure in first-order cerebral arteries (80-100mmHg).

The ends of the arteries were held fixed in the space of the solid model through a non-displacement condition in the structural module.

3.2.5 Fluid-structure interaction

The following boundary conditions were applied to the fluid-structure interaction interface.

The displacements corresponding to the fluid and the solid domain must be compatible, and the mechanical actions are in equilibrium at the fluid/solid limits, and obey the condition of no displacement.⁹³

The ANSYS Workbench software was used to resolve the two-way coupling between the fluid and solid domains. The forces information was first calculated in the Fluent software, and then transferred to the Transient Structural module of ANSYS to determine the mesh displacement information. The mesh displacement information was then transferred back to the Fluent module for the next iteration. When all the iterations converged, the results were analysed and displayed in the ANSYS Results module.

3.2.6 Experiments

In the first study, two scenarios based on arterial segmentations were considered, before and after embolization/clipping of the proximal aneurysm. In 15 cases, it was necessary to perform an idealization of the treatment as there were no post-treatment radiological studies.

The idealization was carried out in the segmentation phase, using the software Slicer 3D, placing an intersection through the major diameter of the aneurysm neck and then smoothing the edges manually. The results of the idealized segmentation were validated by an experienced neurosurgeon or neuroradiologist.

In the second study, the experiment consisted in the application of two profiles in each case, a first profile introducing a delay of 0.2s in blood injection in A1 segment of the non-dominant anterior cerebral artery (asynchronous condition) and a second profile in which there was a simultaneous injection of both A1 segments (synchronous condition) of the anterior cerebral artery.

The third study consisted of full course simulations in two conditions from the same solid. In the first condition (intracranial hypertension) an external pressure of 5223 Pa (equivalent to 40mmHg) was applied to the entire geometry excluding inlets and outlets. For the second condition (low intracranial pressure) an external pressure of 133 Pa (1 mmHg) was applied. The velocity profile of the inlets, the outlets, the thickness of the arterial wall and the characteristics of the fluid were the same in both experiments.

3.3 OUTCOME VARIABLES

3.3.1 Wall shear stress

Wall shear stress (WSS) is a dynamic frictional force induced by viscous fluid moving through the surface of a solid material.⁹⁴ It has been described in several studies as a variable related to trophic changes in the wall of an aneurysm. The aneurysm dome region, the most common site of aneurysm rupture contains areas of low WSS.

This hemodynamic condition is related to mechanobiological phenomena of the endothelium, favouring the degradation of the extracellular matrix, cell death and other inflammatory phenomena leading to destructive remodelling.³

Despite being widely described and related to aneurysmal rupture, WSS is a vector quantity with a very complicated spatial and temporal variation difficult to categorize. For example, there is no single WSS for a given aneurysm, but it varies according to along the cardiac cycle at each specific point in the aneurysm geometry, making it difficult to

homogenize the variable in operational results when trying to compare various studies or methodologies.

Studies that have performed steady-state simulations are comparable to that using temporal-averaging of the WSS (TAWSS),⁸² this variable could be used as a general approximation of WSS behaviour in a given aneurysm,⁹⁵ with the advantage of lower computational effort.

In later studies, some authors have suggested a derived percentage variable that best defines hemodynamic behaviour, the low shear area (LSA), defined as the percentage area of the aneurysm with a WSS less than or equal to 10% of the WSS measured in the efferent artery in a time-averaged fashion.^{96,97} This way, WSS would not be affected by the size of the aneurysm or by the duration of the cardiac cycle.

Figure 3 illustrates a case of the study 1 in which parietal stigmas and its congruence with low shear areas over the aneurysm dome are shown.

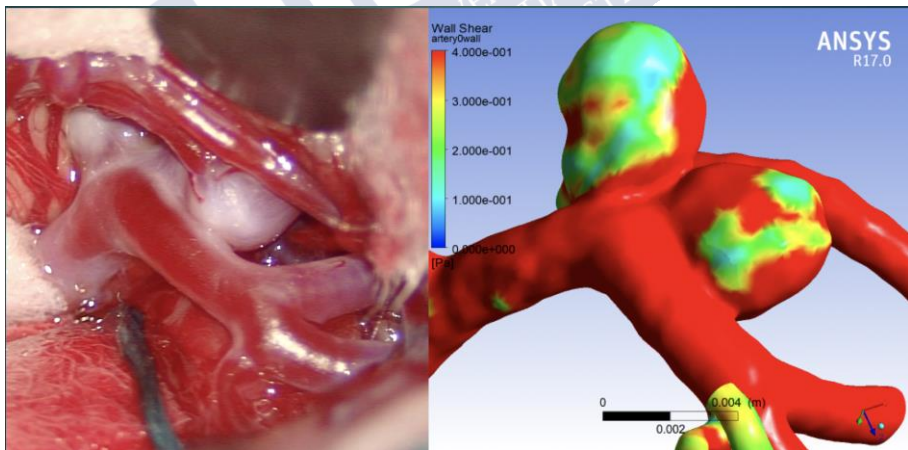


Figure 3. Multiple aneurysms of the middle cerebral artery (unruptured). Left: intraoperative image that shows wall trophic changes in areas of the aneurysm dome. Right: Contours of wall shear stress areas that show some congruence with the intraoperative image.

The role of WSS in the formation and development of aneurysms is complex, since it interacts in different ways at different times in the pathophysiology of aneurysms.

A clear example of this is that geometric and hemodynamic changes are mutually causal, the geometry determines the flow conditions, and the flow changes produces mechanobiological phenomena through inflammatory cascades, which trigger a remodelling of the aneurysm geometry.³ This cycle can become stabilized when hemodynamic conditions are favourable for the blood vessel wall, however, any deviation from these parameters can conduct a destructive cycle that leads to the formation, growth and rupture of aneurysms.

The initial process of aneurysm formation also seems to be governed by hemodynamic phenomena. Acceleration adjacent to arterial bifurcation points produces an environment with high WSS, mechanotransduction phenomena would be related to a biological cascade of aneurysm initiation.⁹⁸⁻¹⁰¹ This cascade would be favoured by an intrinsic or acquired weakness in the arterial wall (for example in smokers) or by altered hemodynamic conditions such as in essential arterial hypertension.^{37,102}

3.3.2 Effective stress and wall displacement

The mechanical properties of cerebral aneurysms were reported by Seshaiyer et al.¹⁰³ Considering the characteristics of the cerebral aneurysm walls confers additional information to hemodynamic phenomena, for this, fluid-structure interaction studies must be used.

Comprehensive descriptions were made by Valencia et al.⁸⁸ In works dealing with these characteristics, the most studied outcome variables are the displacement of the wall (measured in millimetres). This parameter allows the evaluation of the maximum and minimum values, and for different aneurysm locations, such as the neck and dome in a spatial segmentation.

Another important variable consists of the Von-Mises stress, a physical magnitude proportional to the distortion energy, and which

together with the maximum allowable tension of a material is used to predict its mechanical failure, in the case of aneurysms, the rupture.¹⁰⁴ This parameter is often used in order to determine whether a material will yield when subjected to a complex loading situation.

3.3.3 Statistics

All output variables from case-by-case simulations were registered for statistical analysis. For these analyses, SPSS software version 20 for MS Windows was used. The inferential analysis was made from nonparametric tests for dependent samples when comparing among pre and post treatment results, and tests for independent samples when considering ruptured and unruptured aneurysms.

For the study 3, given the small sample, the study used a matching method considering controls with similar characteristics of age, gender and location. We used non-parametric statistical tests to compare groups. A value $p < 0.05$ is assumed to be significant.



4. PUBLISHED ARTICLES

The published articles are accessible through the following links:

4.1 HEMODYNAMIC CHANGES IN THE TREATMENT OF MULTIPLE INTRACRANIAL ANEURYSMS: A COMPUTATIONAL FLUID DYNAMICS STUDY:

<https://doi.org/10.1016/j.wneu.2018.07.009>

4.2 A1 ASYNCHRONY, A POTENTIAL RISK FACTOR FOR THE RUPTURE OF ANTERIOR COMMUNICATING ARTERY ANEURYSMS: A COMPUTATIONAL FLUID DYNAMICS STUDY:

<https://doi.org/10.1016/j.neucir.2019.04.002>

4.3 EFFECTS OF EXTERNAL VENTRICULAR DRAINAGE DECOMPRESSION OF INTRACRANIAL HYPERTENSION ON REBLEEDING OF BRAIN ANEURYSMS: A FLUID STRUCTURE INTERACTION STUDY:

<https://doi.org/10.1016/j.inat.2019.100613>



5. RESULTS

5.1 RISK OF RUPTURE OF MULTIPLE INTRACRANIAL ANEURYSMS AFTER TREATMENT OF A PROXIMAL ANEURYSM

Twenty-four cases were included in the analysis, of these, 20 patients were female (83.33%) and 4 cases were male (16.67%). The average age at diagnosis was 54 years (31 to 75 years). Of the 12 cases of ruptured aneurysms, 10 presented rupture of the proximal aneurysm (83.3%) and two cases presented rupture of the distal aneurysm (16.7%).

All cases of aneurysmal rupture required early treatment of the ruptured aneurysm by endovascular or surgical methods.

Of the patients with ruptured proximal intracranial aneurysms, 9 cases (90%) received treatment of the distal aneurysm, 4 in the first procedure and 5 cases in a deferred procedure. In one case, clinical-radiological follow-up was chosen due to treatment rejection.

In unruptured aneurysms, 7 cases were treated and 5 cases remain under surveillance, to date no bleeding was reported in this group of patients. The characteristics of the population are summarized in Table 4.

Table 4. Baseline characteristics of the study population

Variable	Value	Percentage
<i>Gender (n=24)</i>		
Male	4	16.67%
Female	20	83.33%
<i>Rupture status (n=24)</i>		
Subarachnoid hemorrhage cases	12	50%
Incidental cases	12	50%
<i>Vascular tree(n=24)</i>		
Left carotid tree	18	75%
Right carotid tree	6	25%
<i>Subarachnoid hemorrhage cases (n=12)</i>		
Proximal aneurysm rupture	10	83.33%
Distal aneurysm rupture	2	16.67%
<i>SAH cases - first treatment (n=12)</i>		
Endovascular treatment	8	66.67%
Surgery	4	33.33%
<i>SAH cases - distal aneurysm treatment (n=9) *</i>		
Simultaneous treatment	4	44.44%
Deferred treatment	5	55.56%
<i>Incidental cases (n=12)</i>		
Endovascular treatment	5	41.67%
Surgery	2	16.66%
Follow-up	5	41.67%
<i>Incidental cases - distal an. treatment (n=7)</i>		
Simultaneous treatment	5	71.43%
Staged treatment or single aneurysm treatment	2	28.57%
<i>Interaneurysmal distance (media, DS)</i>	19.35, 8.61	
<i>Size in millimetres (media, DS)</i>		
Ruptured aneurysms (n=12)	7.05, 5.56	
Unruptured aneurysms (n=36)	5.32, 1.95	
Proximal aneurysm (n=24)	6.14, 2.12	
Distal aneurysm (n=24)	5.92, 4.67	

5.1.1 Geometric and hemodynamic analysis of ruptured and unruptured aneurysms

Ruptured aneurysms had an average size of 7.05 mm (SD=5.56mm) and unruptured aneurysms had an average size of 5.23 mm (SD=1.95), ($p=0.035$, Mann Whitney test), the area in the same groups were 296 mm² (SD=58mm²) in broken aneurysms and 61.23 mm² (SD=52.89) in unruptured aneurysms, ($p=0.02$, Mann Whitney test).

The aspect ratio in unruptured aneurysms had a mean of 1.22 (SD=0.36), and in ruptured aneurysms the mean was 2.04 (SD=0.89), ($p=0.001$, Mann Whitney test).

The hemodynamic parameters analysed were the minimum mid-diastole WSS, with values of 0.081 Pa (SD=0.21) in unruptured aneurysms, and 0.009 Pa (SD=0.0001) in ruptured aneurysms, ($p=0.034$, Mann Whitney test).

In systole, maximum peak-systole WSS was considered, the mean value was 49.67 Pa (SD=48.84) in unruptured aneurysms, and 86.88 Pa (SD=29.97) in ruptured aneurysms, ($p=0.04$, Mann Whitney test).

Low shear area (LSA) was 54.67% (SD=29.67) in unruptured aneurysms and 81.81% (SD=16.20) in ruptured aneurysms, ($p=0.296$, Mann Whitney test). The high shear area (HiSA) was 12.87 (SD=14.58) in unruptured aneurysms and 6.54 (SD=7.91) in ruptured aneurysms, ($p=0.51$, Mann Whitney test).

The hemodynamic variables including the low shear area, the high shear area, the minimum mid-diastole WSS, the maximum peak-systole WSS and the maximum pressure in systole are summarized in the table 5.

Table 5. Hemodynamic measurements in ruptured and unruptured aneurysms

	Unruptured aneurysms (mean %, SD) n= 36	Ruptured aneurysms (mean %, SD) n= 12	p-value
LSA	54.67, 29.67	81.81, 16.20	0.296
HiSA	12.87, 14.58	6.54, 7.91	0.51
	Unruptured aneurysms (mean Pa, SD) n= 36	Ruptured aneurysms (mean Pa, SD) n= 12	p-value
Min mid-diastole WSS	0.081, 0.21	0.009, 0.0001	0.034
Max peak-systole WSS	49.67, 48.84	86.66, 29.97	0.04
Max pressure in systole	15019.47, 1627.71	15162.30, 900.50	0.57

The mean interaneurysmal distance was 18.47 mm (range 6 to 31 mm). Additional measurements were made in the distal aneurysm after the treatment of the proximal aneurysm (see Methods).

The pre-treatment minimum mid-diastole WSS had a mean of 0.07 Pa (SD=0.20) and post-treatment of 0.05 Pa (SD=0.11), (p=0.275, Mann Whitney test). The pre-treatment low shear area had a mean of 54.15% (SD=29.19) and post-treatment of 56.39% (SD=28.23), (p=0.02, Mann Whitney test).

Other variables are summarized in Table 6. An illustrative case is presented in Figure 4.

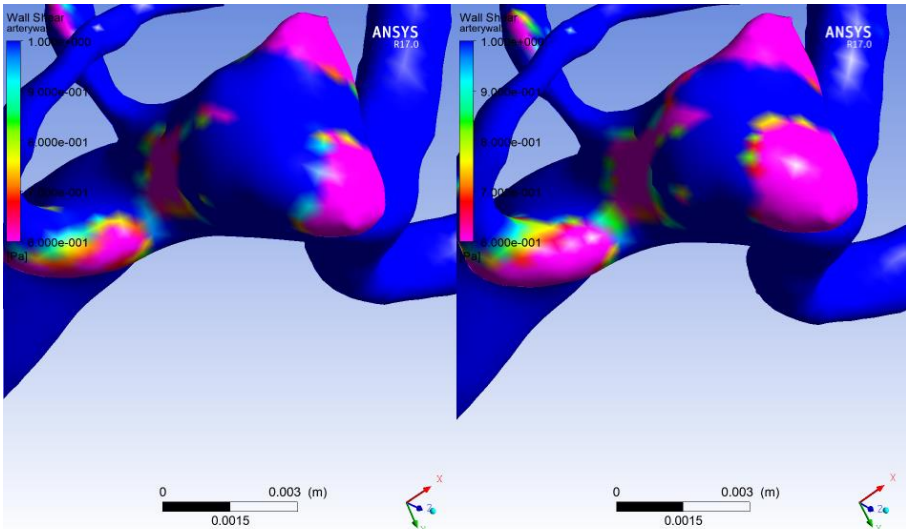


Figure 4. Wall shear stress map in an unruptured middle cerebral artery aneurysm emphasizing the LSA (<0.6 Pa), coexistence of an internal carotid artery aneurysm (not shown). Left: before the treatment of the proximal aneurysm, the LSA is 22.49%. Right: After treatment of the proximal aneurysm, the LSA of the distal aneurysm increased to 38.45%.

Table 6. Hemodynamic effects on the distal aneurysm after treatment of the proximal aneurysm

	Pre-treatment (mean %, SD) n= 24	Post-treatment (mean %, SD) n= 24	p-value
LSA	54.15, 29.19	56.93, 28.23	0.02
HiSA	11.71, 13.49	12.34, 14.15	0.54
	Pre-treatment (mean Pa, SD) n= 24	Post-treatment (mean Pa, SD) n= 24	p-value
Min mid-diastole WSS	0.07, 0.20	0.05, 0.11	0.275
Max peak-systole WSS	52.75, 48.63	61.55, 48.78	0.073
Max pressure in systole	14640, 1580	15031, 1567	0.03

The interaneurysmal distance influences the magnitude of hemodynamic changes in the LSA. A weak positive correlation exists between the interaneurysmal distance and the post-treatment

difference of the LSA ($r=0.26$, $p=0.01$, Pearson correlation). This effect is illustrated in Figure 5. Figure 6 shows the linear regression of this association.

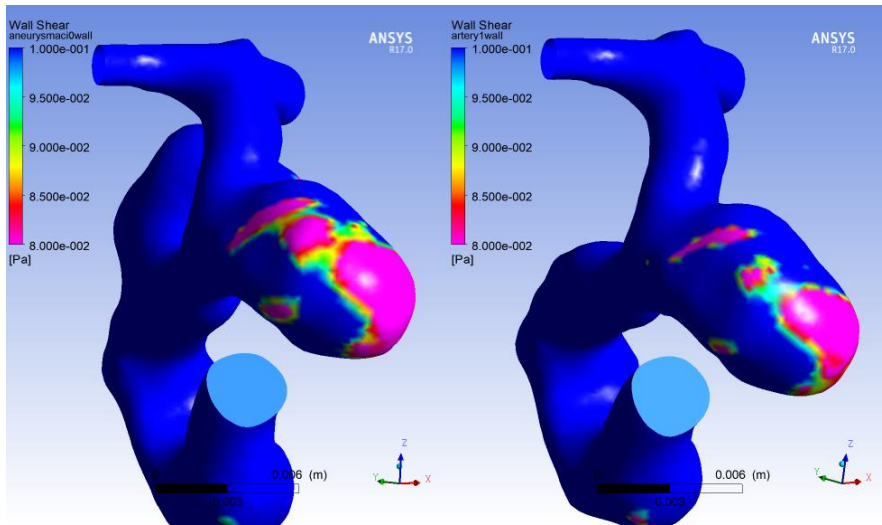


Figure 5. Wall shear stress map in a ruptured aneurysm of internal carotid artery with a second aneurysm at 6 mm in proximal location, the LSA is represented in pink. Left: Before the treatment of the proximal aneurysm LSA is 53%. Right: After treatment of the proximal aneurysm, LSA decreased to 45%.

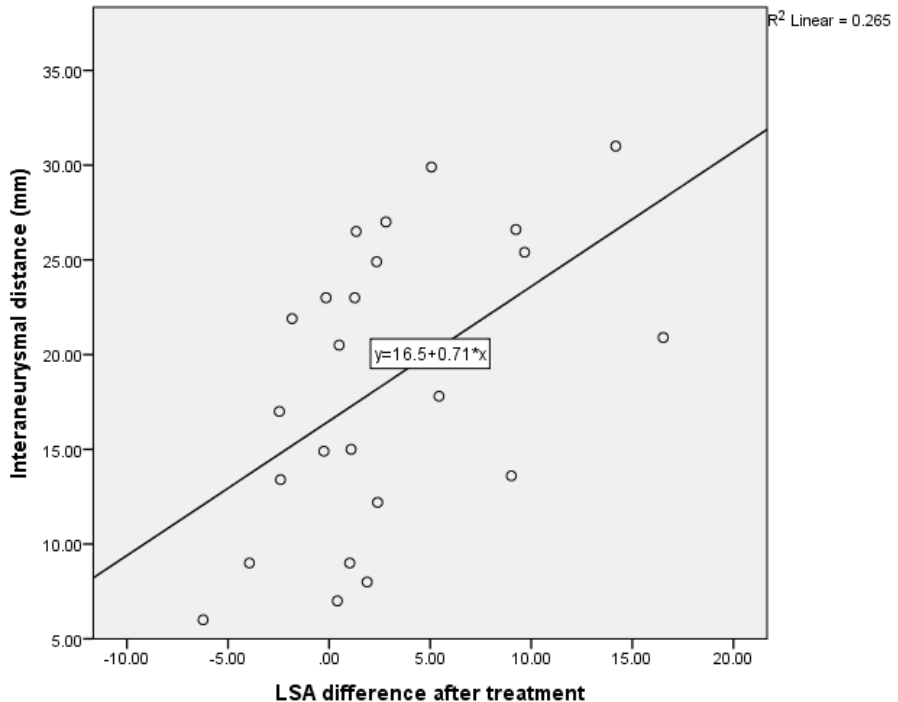


Figure 6. Scatterplot showing the difference in LSA (post-treatment less pre-treatment) and the interaneurysmal distance measured in millimetres.

5.2 EFFECTS OF THE ASYNCHRONY OF A1 ARTERY IN THE HEMODYNAMICS OF ANTERIOR COMMUNICATING ARTERY ANEURYSMS

In this study 54 cases were analysed, 31 of them (57.4%) corresponded to the male gender and 23 cases (42.7%) to the female gender. The mean age of diagnosis was 56 years (SD=14.09). Of these cases, 45 presented as ruptured aneurysms with subarachnoid hemorrhage (83.3%) and 9 cases as unruptured or incidental aneurysms (16.7%).

Considering only the cases of subarachnoid hemorrhage (n=45), the distribution of Fisher's radiological grades was: grade 2 in 10 cases

(22.22%), grade 3 in 16 cases (35.56%), and grade 4 in 19 cases (42.22 %).

In cases of subarachnoid hemorrhage the clinical severity on the WFNS scale was: grade 1 in 22 cases (48.89%), grade 2 in 9 cases (20%), grade 3 in one case (2.22%), grade 4 in 7 cases (15.56%) and grade 5 in 6 cases (13.33%). The characteristics are summarized in table 7.

Table 7. Baseline characteristics of the population in the analysis of anterior communicating artery aneurysms

Variable	Value	Percentage
<i>Gender (n=54)</i>		
Male	31	57.4%
Female	23	42.7%
<i>Rupture status (n=54)</i>		
Subarachnoid hemorrhage cases	45	83.3%
Incidental cases	9	16.7%
<i>SAH cases treatment (n=45) *</i>		
Endovascular	33	61.1%
Surgery	10	18.52
<i>A1 dominance (n=54)</i>		
Left dominance	33	61.11%
Right dominance	21	38.89%
<i>Aneurysm axis lateralization</i>		
Left lateralization	14	25.93%
Right lateralization	40	74.07%

* 2 cases were not treated due to severe hemorrhage with clinical signs of brain stem dysfunction

5.2.1 Geometric and hemodynamic characteristics

Aneurysm measurements were performed including: size, neck dimensions and aspect ratio. A measurement of the diameter of both A1 and A2 arteries, right and left A1/A2 angles, lateralization of the aneurysm and A1-A1 angle were also performed. The geometric characteristics of the anterior communicating complex are described in Table 8.

Table 8. Geometric characteristics of arteries and aneurysms of the anterior communicating complex included in the study

Variable	Minimum	Maximum	Mean	SD
Aneurysm Height (mm)	2.60	14.30	6.54	3.01
Aneurysm Neck (mm)	1.46	7.94	3.53	1.23
Aspect Ratio	0.63	3.87	1.90	0.68
Left A1 diameter (mm)	0.9	2.9	1.76	0.47
Right A1 diameter (mm)	0.9	2.8	1.57	0.49
Left A2 diameter (mm)	0.8	2.4	1.58	0.34
Right A2 diameter (mm)	0.8	2.5	1.52	0.38
Left A1-A2 angle (mm)	18.90	159.60	86.98	34.37
Right A1-A2 angle (mm)	2.3	160.60	78.25	37.47
A1-A1 angle (degrees)	56.50	176.80	136.12	27.37
Symmetry index	0.39	0.94	0.67	0.15

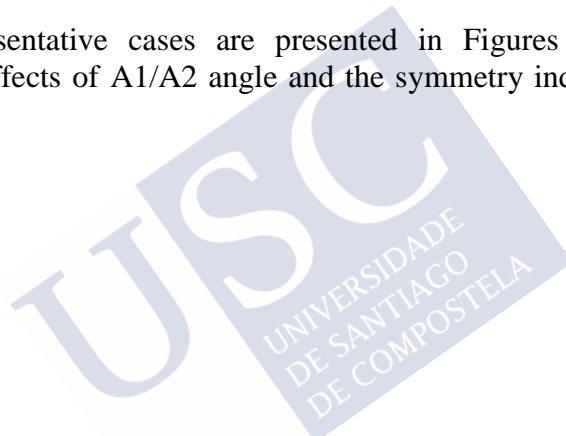
Time-averaged wall shear stress (TAWSS) had a mean of 1.25 Pa in asynchronous conditions and 1.34 Pa in synchronous conditions ($p=0.05$, paired sample t-test), the time-averaged mean pressure had an average of 13205 Pa and 13495 Pa in conditions of asynchrony and synchrony respectively ($p=0.004$, paired sample t-test).

The difference produced in LSA in conditions of synchrony and asynchrony resulted in a wide difference of positive and negative values (from -35.68 to 27.34). For this reason, we categorized the population into two groups, LSA increased in asynchrony and LSA decreased in asynchrony. Table 9 shows the effect of different variables with respect to this phenomenon in a univariate analysis. In this analysis, only the symmetry index and the dominant A1/A2 angle were related to LSA changes.

Table 9. Univariate analysis of the low shear area in relation to the geometric characteristics of the anterior communicating complex

Variable	LSA increase (n= 31)	LSA decrease (n=23)	p-value
Mean aneurysm height (mm)	5.99	6.72	0.99
Mean aneurysm neck (mm)	3.57	3.43	0.55
Mean Aspect ratio	1.72	2.01	0.28
Mean A1-A1 angle (degrees)	139.49	137.48	0.70
Dominant side A1-A2 angle (degrees)	63.12	91.14	0.04
Mean symmetry index	0.72	0.62	0.04

Two representative cases are presented in Figures 7 and 8 regarding the effects of A1/A2 angle and the symmetry index on the low shear area.



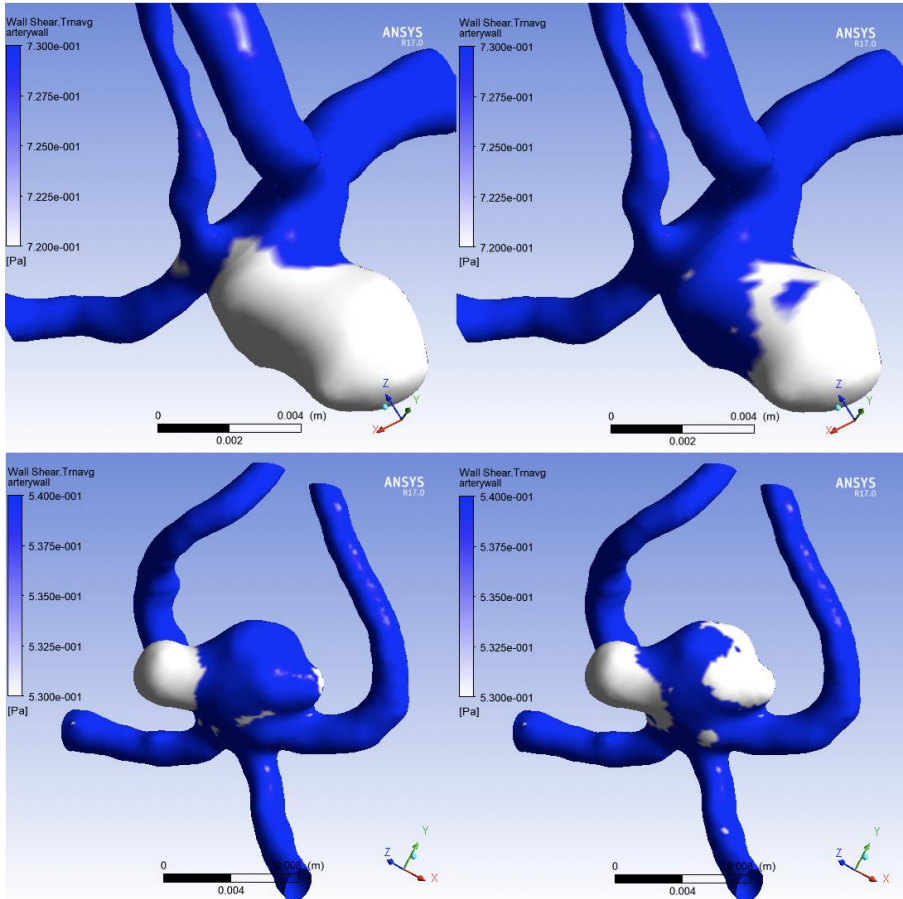


Figure 7. Low shear area (white) in anterior communicating aneurysms in synchrony and asynchrony conditions. Upper row: left figure shows a right A1 hypoplasia with a symmetry index of 0.39 in synchrony conditions, right figure shows the same in asynchrony conditions; LSA decreased from 50.93 to 26.40 considering asynchrony condition. Lower row: left figure shows a right dominant A1 segment, symmetry index is 0.9, right figure shows the same aneurysm in asynchrony conditions, LSA increased from 25.03 to 36.78.

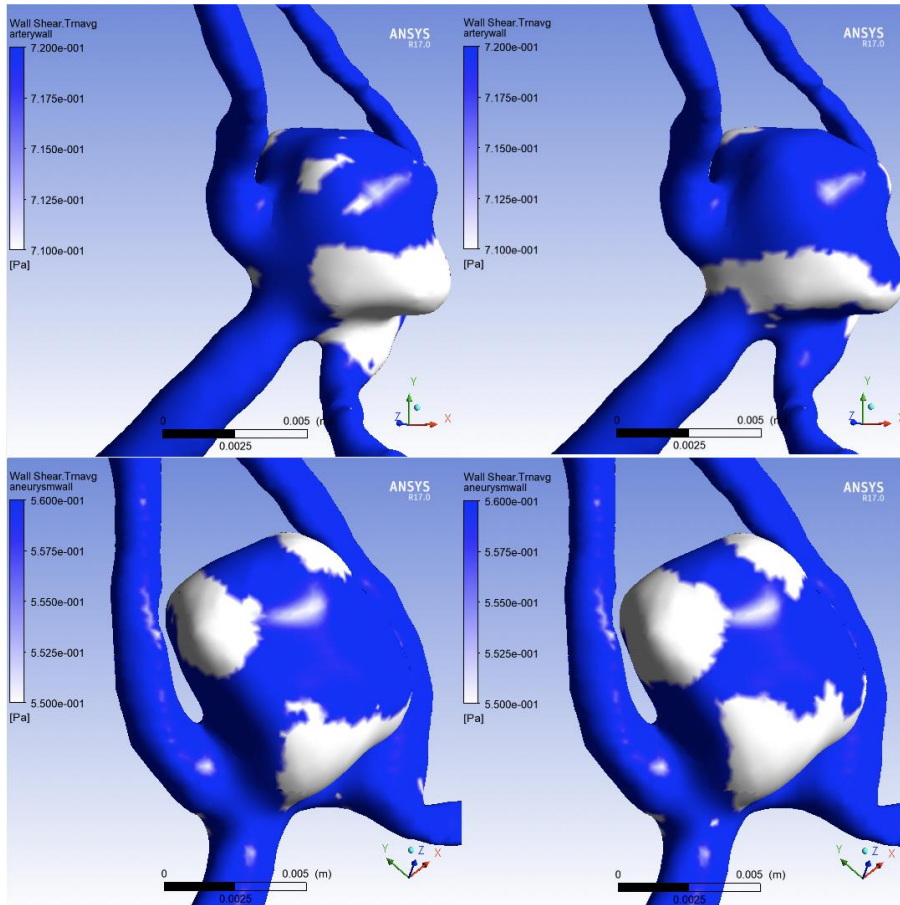


Figure 8. Low shear area (white) in anterior communicating aneurysms in synchrony and asynchrony conditions. Upper row: left figure shows a dominant A1/A2 angle of 88.62 degrees in synchronic conditions, right figure shows the same aneurysm in asynchrony conditions; LSA decreased from 31.64 to 26.06. Lower row: left figure shows a dominant A1/A2 angle of 46.45 degrees in synchronic conditions, right figure shows the same aneurysm in asynchrony; LSA increased from 27.69 to 36.95.

The effects of asynchrony on intra-aneurysmal pressure was mainly negative with a mean of -289 Pa (range of -4755.84 to 218.10 Pa, SD=717.16 Pa)

5.3 GEOMETRIC AND HEMODYNAMIC EFFECTS OF INTRACRANIAL PRESSURE REDUCTION BY EXTERNAL VENTRICULAR DRAINAGE IN THE REBLEEDING PHENOMENON

A fluid-structure interaction method was used for this study. Geometric variables such as height, neck, aspect ratio and clinical characteristics are summarized in Table 10.

Table 10. Demographic, clinical and geometric variables grouped by rebleeding

	Gender (F:M)	Age (mean, SD)	Height (mean, SD)	Neck (mean, SD)	Aspect ratio (mean, SD)	WFNS score (mean, SD)
Rebleeding	4:2	53.33, 13.18	7.36, 1.15	3.4, 0.32	1.93, 0.26	4.66, 0.51
No rebleeding	9:3	51.58, 12.64	6.55, 1.44	3.11, 0.52	1.97, 0.39	4.33, 0.65

5.3.1 Wall displacement

There is a positive aneurysmal wall displacement during the systolic phase of the cardiac cycle. Two conditions were simulated, with high intracranial pressure and low intracranial pressure. In cases of intracranial hypertension, the maximum displacement of wall in systole in aneurysms that presented rebleeding was 0.34 mm (SD=0.28), and in aneurysms that did not rebleed 0.36mm (SD=0.29), ($p=0.055$, Mann Whitney test).

The difference in displacement before and after the placement of an external ventricular drainage (HICP-LICP) was calculated, this value had a mean of 0.01567 mm (SD=0.007) in aneurysms that presented rebleeding and 0.00683 mm (SD=0.005) in aneurysms that did not show rebleeding ($p=0.05$, Mann Whitney test).

The rupture site usually coincides with the low shear area. Wall displacement measurements were performed exclusively in this low shear area. The differential magnitude of measurements in high and low

intracranial pressure was 0.026 mm (SD=0.005) in aneurysms that presented rebleeding and 0.0065 mm (SD=0.002) in aneurysms that did not show rebleeding after the placement of an external ventricular drainage (p=0.01, Mann Whitney test). Two representative cases regarding this interaction are presented in Figures 9 and 10

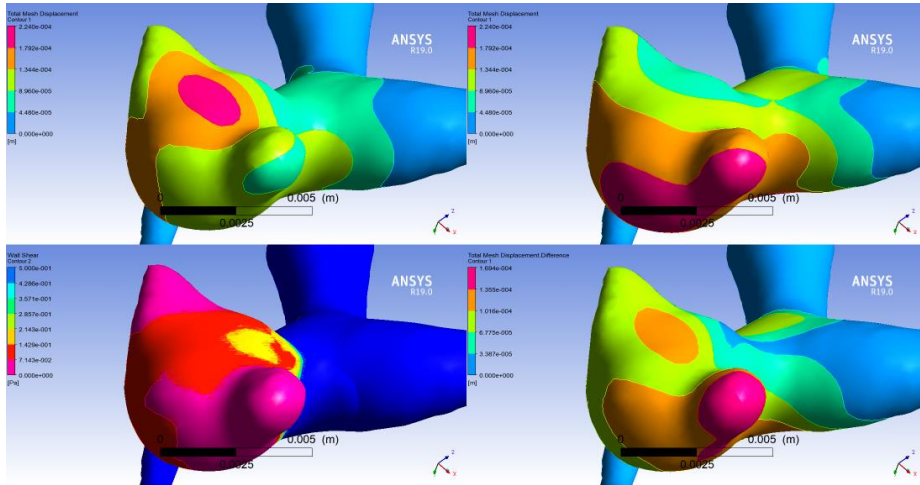


Figure 9. Wall Displacement and WSS relations in a rebleeding aneurysm case. Upper left: Wall displacement contours before the placement of the EVD. Upper right: Wall displacement contours after the placement of EVD. Lower left: Mid-diastolic WSS showing areas of low stress in two regions of the dome. Lower right: Displacement differences after EVD placement, note congruence with LSA region in an aneurysmal bleb.

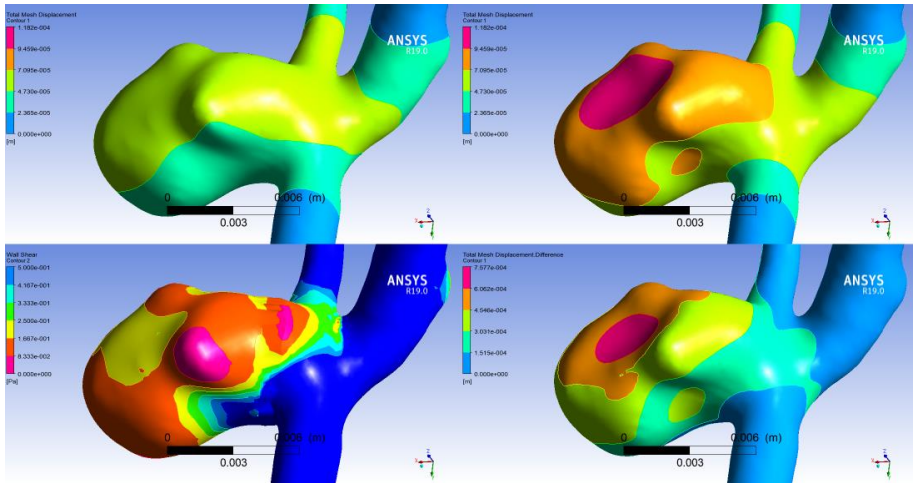


Figure 10. Wall Displacement and WSS relations in an aneurysm with no rebleeding after EVD. Upper left: Wall displacement contours before the placement of the EVD. Upper right: Wall displacement contours after the placement of EVD. Lower left: Mid-diastolic WSS showing areas of low stress in one region of the dome. Lower right: Displacement differences after EVD placement, note incongruence with LSA region, more displacement was measured in an area distant from LSA.

5.3.2. Von Mises stress

The distribution of Von Mises stress, or effective stress, had a mean of 4.77 MPa (SD=2.67) in aneurysms that rebleed and 3.26 MPa (SD=1.37) in aneurysms that did not rebleed ($p=0.25$, Mann Whitney test). Under conditions of low intracranial pressure, aneurysms that rebleed had a mean of 2.28 MPa and aneurysms that did not rebleed had a mean of 1.42 MPa, ($p=0.33$, Mann Whitney test).

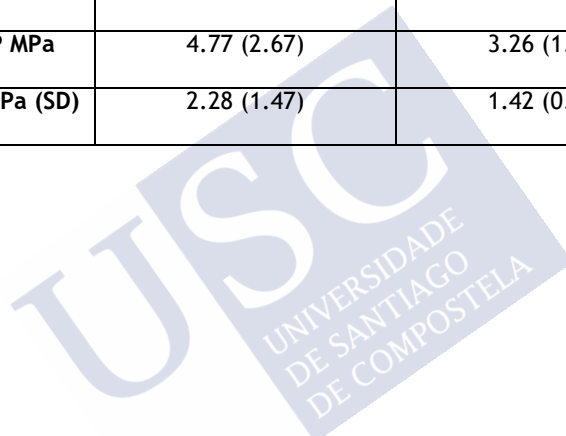
5.2.3 Wall shear stress

Time-averaged wall shear stress under conditions of elevated intracranial pressure had an average of 1.177 Pa in aneurysms that presented rebleeding and 1.2192 Pa in aneurysms that did not show rebleeding ($p=0.75$, Mann Whitney test). Under conditions of low intracranial pressure, the average of this variable was 1.17775 Pa in aneurysms that presented rebleeding and 1.2125 Pa in aneurysms that did not show rebleeding ($p=0.75$, Mann Whitney test).

A summary of all geometric and hemodynamic variables is presented in table 11.

Table 11. Geometric and hemodynamic changes before and after the placement of an external ventricular drainage, grouped by the state of rebleeding

	Rebleeding	No rebleeding
TAWSS, HICP, Pa (SD)	1.1767 (0.30)	1.2192 (0.34)
TAWSS, LICP, Pa (SD)	1.1775 (0.30)	1.2125 (0.34)
Displacement, HICP, mm (SD)	0.34 (0.28)	0.26 (0.10)
Displacement, LICP, mm (SD)	0.36 (0.29)	0.27 (0.10)
Von Mises HICP MPa (SD)	4.77 (2.67)	3.26 (1.37)
Von Mises LICP MPa (SD)	2.28 (1.47)	1.42 (0.94)



6. DISCUSSION

6.1 MULTIPLE INTRACRANIAL ANEURYSMS: HEMODYNAMIC EFFECT OF THE TREATMENT OF PROXIMAL INTRACRANIAL ANEURYSMS.

Multiple intracranial aneurysms are present in 15 to 35% of cases of subarachnoid hemorrhage.¹⁰⁵ Its presence is independently associated with higher mortality, rebleeding and occurrence of early rebleeding.¹⁰⁶ Additionally, the Korean Clinical Practice Guidelines for Aneurysmal Subarachnoid Hemorrhage recommends the treatment of multiple intracranial aneurysms whenever feasible as it reduces the risk of selection error.¹⁰⁷

Few studies have evaluated the hemodynamics of multiple intracranial aneurysms.¹⁰⁸⁻¹¹⁰ Furthermore, we did not find previous studies that describe the hemodynamic behaviour before and after the treatment of multiple aneurysms. Castro et al,¹¹¹ highlighted the importance of afferent artery segmentation in studies of computational fluid dynamics. Therefore, it is expected that hemodynamic changes could be produced by the embolization of a single proximal aneurysm.

In our study, as in previous studies, the aspect ratio and aneurysm size was significantly higher in ruptured aneurysms.¹¹² Hemodynamic analysis showed profiles of a larger low shear area, maximum peak-systole WSS, and minimum mid-diastole WSS in ruptured aneurysms.

In this study, nine post-treatment cases and fifteen idealized cases of proximal aneurysm treatment were analysed. After treatment of the proximal aneurysm, the distal aneurysm showed a hemodynamic profile of increased bleeding risk if the theory of low wall shear stress is considered valid as predisposing to the aneurysmal rupture event.

After the treatment of the proximal aneurysm the low shear area and the maximum peak-systole WSS are significantly higher. The impact of this association is illustrated in Figure 4.

The low shear area is directly proportional to the inter-aneurysmal distance. This relationship is opposite in patients with distances inferior to 10 mm between both aneurysms, in which the LSA decreases. This phenomenon is shown in Figure 5. The proximity between aneurysms in this scenario could improve the trophic conditions of the wall by reducing damage and remodelling of the arterial wall mediated by the WSS.⁸

Although the hemodynamic conditions of a distal aneurysm appear to become favourable if the interaneurysmal distance is less than 10 mm, it is often difficult to identify the ruptured aneurysm in patients with multiple aneurysms and subarachnoid hemorrhage, and it would be much even more difficult in patients with short interaneurysmal distances.

To avoid selection errors in the treatment of ruptured aneurysms, the current tendency is to treat all of them in a single session whenever possible, in this scenario surgery presents a disadvantage compared to endovascular methods (cerebral oedema, hydrocephalus and need for extensive dissections).¹¹³

In our case series, most distal aneurysms were treated in a second procedure. In 3 cases, it was considered that the ruptured aneurysm was clearly the proximal one and that the distal aneurysm did not present high-risk characteristics (i.e. height less than 7 mm), the attending physician considered that the morbidity could be reduced by treating the distal aneurysm in a deferred form, after clinical stabilization of the acute haemorrhagic event.

In 2 cases, the neurosurgeon considered that the treatment of the distal aneurysm could represent an increased risk of morbidity if performed in the same procedure, one of these cases was treated later with surgery and another by endovascular procedures. Four cases were treated in the same procedure.

In total, 9 patients received treatment and a single case remains untreated, a 65-year-old patient with a 4.7 mm middle cerebral artery aneurysm, the patient's functional status is bad (severe disability) and her family rejects treatments, the patient is still followed with periodic radiological-clinical assessments.

6.2 THE ASYNCHRONY OF THE A1 SEGMENT IN THE RISK OF RUPTURE OF ANTERIOR COMMUNICATING ARTERY ANEURYSMS

The anatomical configuration of the human arterial system determines that with each cardiac cycle, four different waves reach the Willis circle at different times. The first branch of the aortic arch is the brachiocephalic trunk, which branches into the right common carotid artery and right subclavian artery, on the left side the common carotid artery and the subclavian artery arise independently and directly from the aortic arch. This particular asymmetric configuration and other pathological variants such as the existence of atherosclerotic plaques determine that the brain pulse is asynchronous.¹¹⁴

The anterior communicating artery is a complex site due to its anatomical characteristics. This artery receives flow from two completely independent circulations; In addition, the diameters of both anterior cerebral arteries are usually different in patients with intracranial aneurysms. Several studies have identified that the configuration of the anterior communicating complex is a risk factor for the development and rupture of intracranial aneurysms, and also increases the risk of complications derived from the treatment of aneurysms at this location.¹¹⁵⁻¹¹⁷

Zhang et al,¹¹⁸ analysing 655 cases with aneurysms in different locations described that the A1/A2 angle is lower in individuals with anterior communicating artery aneurysms, with an average of 106 degrees compared to 120 degrees in the group that do not have aneurysms in this location. In our series, the angle A1/A2 was smaller, reaching an average of 82 degrees. The previous study also finds that there is a lateralization of the anterior communicating seeding towards

the side that offers a smaller A1/A2 angle, this finding is comparable with our findings.

Lin et al,¹¹⁹ analysing 79 cases of anterior communicating artery aneurysms described lower dominant A1/A2 angles in patients with ruptured aneurysms at this location, other studies found similar results.^{120,121} In our study, no significant association was found in this variable, although it should be considered that only nine patients with unruptured aneurysms were analysed in our study.

Hemodynamic conditions play an important role in the pathophysiology of aneurysm formation, growth and rupture. The most described variable is wall shear stress, defined as the frictional force exerted by the blood flow tangentially in the light of the vessel. This variable is usually diminished in ruptured aneurysms, highlighting its potential role in the event of rupture.¹²² Low shear area was also described in many studies as a correlate of a low wall shear stress, this variable is defined as the percentage of the aneurysmal surface that is subjected to a wall shear stress lower than 10% of the afferent artery.⁹⁶

In our study, there is a significant direct influence of the asynchronous pulse in the A1 artery in the hemodynamic conditions of the aneurysm, including a reduction in total pressure and changes in time-averaged wall shear stress, which are reflected in two groups. Some aneurysms showed an increase in TAWSS and a decrease in the low shear area, and others behaved in the opposite way.

In the univariate analysis, higher symmetry rates and lower A1/A2 angles were associated with an increase in the low shear area, thus increasing their theoretical risk of bleeding under asynchronous conditions.

The effect of asynchronous pulses can produce a decrease in TAWSS when A1 diameters are symmetric. Considering that two significant flows produce a complex interaction resulting in an additive effect on the aneurysmal TAWSS over the entire cardiac cycle, this effect would not be achieved with asynchrony, and therefore TAWSS would decrease increasing low shear area.

On the other hand, in the presence of larger A1/A2 angles in the dominant artery, more blood volume would be directed directly to the A2 segments without interacting with the aneurysm. The synchrony can play a role stabilizing intra-aneurysmal flow and providing an effective trophic WSS, that in conditions of asynchrony, would be insufficient and reduced. This phenomenon becomes more significant when the angle A1/A2 is reduced.

In addition to the geometric characteristics described above, and associated with an increase in the incidence of aneurysms at this location, asynchrony could play an important role in the formation and growth of aneurysms. Therefore, these variables should be considered in subsequent studies that evaluate the hemodynamics of this complex location.

6.3 EFFECTS OF THE DECOMPRESSION OF INTRACRANIAL HYPERTENSION ON THE REBLEEDING OF CEREBRAL ANEURYSMS

In this study, the structural and hemodynamic changes that occur in intracranial aneurysms that presented rebleeding after implantation of an external ventricular drainage were evaluated. These cases were matched with aneurysms that did not bleed after the same procedure.

All aneurysms included in this study were initially ruptured aneurysms. The dimensions and aspect ratio did not show significant differences comparing the rebleeding and non-rebleeding groups, as expected by the matching methodology. Most studies of this nature describe Von Mises stress and WSS as the main variables of study. The findings of our study are compatible with previous studies that analysed the same variables in intracranial aneurysms.¹²³

Wall shear stress has been described in several studies as a variable related to trophic changes in the wall of an aneurysm. The aneurysm dome region, the most frequent site of rupture, contains areas of low WSS. This hemodynamic condition is related to mechanobiological phenomena of the endothelium, which favour the degradation of the

extracellular matrix, promote cell death and other inflammatory phenomena leading to a destructive remodeling.³ It is assumed that 2 Pa of WSS would be sufficient to promote sufficient structure and strength in the wall of an aneurysm.¹²⁴

If we consider the rebleeding phenomenon after the placement of an external ventricular drainage, TAWSS does not show significant differences in both conditions, probably because all aneurysms in our study share a common initial characteristic, they are ruptured aneurysms. On the other hand, the scarce effect of geometric changes in relation to the velocity profile usually leads to insignificant changes in the WSS in cases of arterial hypertension,¹²⁵ and a similar effect is expected by increasing intracranial pressure.

Although TAWSS is similar in both groups, certain areas of the aneurysm with low TAWSS may contain areas of trophic changes that predispose the aneurysm to rupture even with minimal changes of wall displacement or effective stress.

According to MacDonald et al,¹²⁶ the rupture stress of an aneurysm varies between 0.73 and 1.91 MPa. In our study, the effective tensions of 2.28 MPa during systole, after the placement of an external ventricular drainage, and compared with 4.77 MPa before the procedure, suggest that intracranial pressure plays an important role in rupture stress. However, the haemostatic effect that is obtained with intracranial hypertension, either by a hematoma or by hydrocephalus, would be more relevant in the rebleeding process of an aneurysm. In addition, lower effective stress after decompression in aneurysms that did not rebleed, which in our study reaches 1.42 MPa, could explain why these aneurysms did not rebleed after decompression.

Although the neck of an aneurysm has the highest effective stress of all geometry,⁸⁸ the preferential location of degenerative wall changes that contribute to aneurysmal rupture are located in the aneurysm dome,^{127,128} increasing the susceptibility to rupture in this site.

At present, it is very difficult to establish the characteristics of the material and thickness in specific areas of the wall of an aneurysm for studies of fluid-structure interaction. Some studies analysed materials

obtained through surgeries or autopsy pieces, but currently there is no medical technology in neuroimaging that has spatial and temporal resolution enough to determine this information in vivo and allows it to be transferred to clinical practice.¹²⁹ Therefore, in these studies we assume that low shear areas correspond to potential rupture sites,¹²⁸ changes in effective stress and displacement over these areas could determine the failure of the material more easily, causing the rupture of the intracranial aneurysm.

In our study, an increase in wall displacement was found after implantation of external ventricular drainage in patients who rebleed. After the placement of an external ventricular drainage, the hot spots of maximum wall displacement of an aneurysm seem to move to other areas of the aneurysm geometry (See figures 9 and 10). One of the main findings of our study suggests that an increase in wall displacement in low shear areas has a stronger association with rebleeding than wall displacement in the complete geometry of the aneurysm.

The role of elevated intracranial pressure in patients with subarachnoid hemorrhage, either due to acute hydrocephalus or due to hematoma mass effect, is of great importance in hemodynamic changes. Intracranial hypertension could contribute to an arrest of aneurysmal bleeding, as it seems intuitive and has been discussed in previous studies.¹³⁰ A greater maximum wall displacement was found in low shear areas in cases of rebleeding compared to control cases. This suggests that the significant reduction in intracranial pressure (40 mmHg or 5332 Pa) that occurs after placing an external ventricular drainage would cause the reopening of the initial rupture site, cancelling the haemostatic effect of intracranial hypertension, rather than causing a new rupture in the aneurysmal wall. Considering this discussion in cases of multiple intracranial aneurysms with the ruptured aneurysm already treated, procedures that reduce intracranial pressure could be considered safe for unruptured aneurysms.

This doctoral thesis presented extensively the findings published in previous articles.¹³¹⁻¹³³

6.4 LIMITATIONS

A large part of the assumptions of the individual conclusions of the studies presented here assume the theory of wall shear stress as true in the genesis, progression and final evolution in the pathophysiology of intracranial aneurysms.

Although many studies assessed CFD in aneurysms before, there is still an open discussion about the role of hemodynamic in the inflammatory response; for example, the role of high and low wall shear stress in the phenomenon of aneurysmal rupture remains to be established. It's still unknown the role of the geometric changes of the aneurysm after rupture. This is a very relevant fact since a large part of the assumptions come from studies carried out after the rupture event. It is still unknown what will be the meaning of the variables resulting from computational fluid dynamics studies and what will be the clinical translation of them, taking into account that most intracranial aneurysms will never rupture.

The retrospective characteristics of our studies also represent a limitation, under ideal conditions. Certain specific variables of the patients such as the arterial velocity profile of the inlets, perfusion studies, narrow and detailed clinical follow-up, and systematization of the moments of data collection are absent in retrospective records and could be achieved through prospective methodologies.

7. CONCLUSIONS

- Hemodynamic changes in the distal aneurysm after treatment of the proximal aneurysm in cases of multiple intracranial aneurysms show an unfavourable risk profile, increasing the theoretical risk of aneurysm bleeding. This finding reinforces the paradigm of simultaneous treatment of multiple aneurysms whenever possible, even the unruptured ones.
- The asynchrony in the flow of the A1 segments of the anterior cerebral artery produces unique hemodynamic changes in aneurysms of the anterior communicating artery, there is an increase in the low shear area in the absence of asymmetry of A1 and higher A1/A2 angles, potentially increasing the risk of rupture in aneurysms of this location.
- Using fluid-structure interaction simulations, structural and hemodynamic changes in relation to aneurysmal rebleeding after the placement of an external ventricular drainage include: an increase in wall displacement throughout the cardiac cycle. Differences in wall displacement in low shear areas are strongly associated with rebleeding of aneurysms in our series.



8. ANNEXES





8.1 STATEMENT OF THE RESEARCH ETHICS COMMITTEES OF GALICIA



Secretaría Técnica
Comité Autonómico de Ética da Investigación de Galicia
Secretaría Xeral, Concellería de Sanidade
Edificio Administrativo San Lázaro
15703 SANTIAGO DE COMPOSTELA
Tel: 981546425. Correo-e: caic@sergas.es



DICTAMEN DEL COMITÉ DE ÉTICA DE LA INVESTIGACIÓN DE PONTEVEDRA-VIGO-ORENSE

María Asunción Verdejo González, Secretaria del Comité de Ética de la Investigación de Pontevedra-Vigo-Ourense

CERTIFICA:

Que este Comité evaluó en su reunión del día 17/04/2018 el estudio:

Título: Análisis geométrico y hemodinámico del riesgo de ruptura en aneurismas intracraneales

Versión: revisión 2

Promotor: José Luis Thenier Villa

Investigador: José Luis Thenier Villa

Código de Registro: 2018/053

Y que este Comité, tomando en consideración la pertinencia del estudio, el conocimiento disponible, los requisitos éticos, metodológicos y legales exigibles a los estudios de investigación con seres humanos, sus muestras o registro y los procedimientos normalizados de trabajo del Comité, emite un dictamen **FAVORABLE** para la realización del citado estudio.

Y HACE CONSTAR QUE:

1. El Comité Territorial de Ética de la Investigación de Pontevedra-Vigo-Ourense cumple tanto en su composición, como en sus procedimientos normalizados de trabajo, los requisitos legales vigentes.
2. La composición actual del Comité Territorial de Ética de la Investigación de Pontevedra-Vigo-Ourense es:
 - **D. Alfonso Casas Losada (Presidente)**. Médico especialista en Psiquiatría.
 - **D^a. Iria Aparicio Rodríguez (Vicepresidenta)**. Médica especialista en Obstetricia y Ginecología.
 - **D^a. Asunción Verdejo González (Secretaria)**. Médica Especialista en Farmacología Clínica.
 - **D. Víctor del Campo Pérez (Secretario Suplente)**. Médico Especialista en Medicina Preventiva y Salud Pública.
 - **D^a. Marisol Aira Quintela**. Médica Especialista en Medicina Familiar y Comunitaria.
 - **D. Jorge Luis Arias Otero**. Licenciado en Físicas.
 - **D^a. María de las Mercedes Guerra García**. Farmacéutica de Atención Primaria.
 - **D. Adolfo Paradela Carreiro**. Farmacéutico de Atención Especializada.
 - **D^a. María Eva Pérez López**. Médica Especialista en Oncología Médica.
 - **D^a. María Ponte García**. Licenciada en Derecho.
 - **D. Juan Carlos Rodríguez García**. Médico Especialista en Medicina Interna.
 - **D^a. Cristina Torreira Banzas**. Médica Especialista en Análisis Clínicos.
 - **D^a. Miriam Vázquez Campo**. Diplomada Universitaria de Enfermería.

Para que conste donde proceda, y a petición de quien proceda,

En Vigo, a 20 de Abril de 2018.

Nombre de reconocimiento (DN):
c=ES, serialNumber=13768463L,
sn=VERDEJO GONZALEZ,
givenName=MARIA ASUNCION,
cn=VERDEJO GONZALEZ MARIA
ASUNCION - 13768463L
Fecha: 2018.04.20 12:27:38
+02'00'

8.2 INFORMED CONSENT (ORIGINAL IN SPANISH)

HOJA DE INFORMACIÓN AL/LA PARTICIPANTE ADULTO/A

TÍTULO DEL ESTUDIO: Análisis geométrico y hemodinámico del riesgo de ruptura en aneurismas intracraneales

INVESTIGADOR:...Dr. José Luis Thenier Villa

CENTRO: Hospital Álvaro Cunqueiro de Vigo

Este documento tiene por objeto ofrecerle información sobre un **estudio de investigación** en el que se le invita a participar. Este estudio fue aprobado por el Comité de Ética de la Investigación de Pontevedra-Vigo-Ourense

Si decide participar en el mismo, debe recibir información personalizada del investigador, **leer antes este documento** y hacer todas las preguntas que precise para comprender los detalles sobre el mismo. Se así lo desea, puede llevar el documento, consultarlo con otras personas, y tomar el tiempo necesario para decidir si participa o no.

La participación en este estudio es completamente **voluntaria**. Ud. puede decidir no participar o, se acepta hacerlo, cambiar de parecer retirando el consentimiento en cualquier momento sin dar explicaciones. Le aseguramos que esta decisión no afectará a la relación con su médico ni a la asistencia sanitaria a la que Ud. tiene derecho.

¿Cuál es el propósito del estudio?

Analizar a partir de los estudios radiológicos llevados a cabo con respecto a su enfermedad (TAC, resonancias, arteriografías...) en búsqueda de características estructurales específicas que puedan explicar, por qué algunos aneurismas cerebrales se rompen causando hemorragias y otros permanecen estables durante el tiempo.

¿Por qué me ofrecen participar a min?

Ud. es invitado a participar porque *padece o ha padecido la enfermedad objetivo del estudio, el aneurisma intracraneal.*

¿En que consiste mi participación?

Se revisarán su historia clínica y se utilizarán sus pruebas radiológicas y otros datos poblacionales como su género, edad, etc. Al tratarse de un estudio de revisión de hechos del pasado, su seguimiento habitual y su manejo en el futuro no se verá afectado por participar en este estudio

Su participación tendrá una duración total estimada menor de 2 minutos *No será necesaria su participación directa en el estudio, aunque si existiera algún dato imprescindible que no se encuentre registrado en su historia clínica y sea de importancia para el estudio, el investigador podrá ampliar la anamnesis dirigiéndole preguntas sencillas en sus revisiones.*

¿Qué molestias o inconvenientes tiene mi participación?

Su participación no implica molestias adicionales a las de la práctica asistencial habitual

Versión: [2], data [Abril/2018]

Se deberán firmar dos modelos, uno será entregado al participante y otro será conservado por el responsable del estudio de investigación

¿Obtendré algún beneficio por participar?

No se espera que Ud. obtenga beneficio directo por participar en el estudio. La investigación pretende descubrir aspectos desconocidos o poco claros sobre los aneurismas intracraneales. Esta información podrá ser de utilidad en un futuro para otras personas.

¿Recibiré la información que se obtenga del estudio?

Se Ud. lo desea, se le facilitará un resumen de los resultados del estudio.

¿Se publicarán los resultados de este estudio?

Los resultados de este estudio serán remitidos a publicaciones científicas para su difusión, pero no se transmitirá ningún dato que pueda llevar a la identificación de los participantes.

¿Cómo se protegerá la confidencialidad de mis datos?

El tratamiento, comunicación y cesión de sus datos se hará conforme a lo dispuesto por la Ley Orgánica 15/1999, de 13 de diciembre, de protección de datos de carácter personal. En todo momento, Ud. podrá acceder a sus datos u oponerse, solicitando ante el investigador

Solamente el equipo investigador, y las autoridades sanitarias, que tienen deber de guardar la confidencialidad, tendrán acceso a todos los datos recogidos por el estudio. Se podrá transmitir a terceros información que no pueda ser identificada. En el caso de que alguna información sea transmitida a otros países, se realizará con un nivel de protección de los datos equivalente, como mínimo, al exigido por la normativa de nuestro país.

Sus datos serán recogidos y conservados hasta terminar el estudio de modo:

- **Codificados**, que quiere decir que poseen un código con el que el equipo investigador podrá conocer a quien pertenece.

El responsable de la custodia de los datos es el *Dr. José Luis Thenier Villa*. Al terminar el estudio los datos serán anonimizados

¿Existen intereses económicos en este estudio?

Esta investigación es promovida por el primer autor del estudio, no existe una aportación de fondos de terceros para esta investigación.

El investigador no recibirá retribución específica por la dedicación al estudio.

Ud. no será retribuido por participar. Es posible que de los resultados del estudio se deriven productos comerciales o patentes. En este caso, Ud. no participará de los beneficios económicos originados.

¿Cómo contactar con el equipo investigador de este estudio?

Ud. puede contactar con José Luis Thenier Villa en el teléfono +34622597286 o el correo electrónico jose.luis.thenier.villa@sergas.es

Muchas Gracias por su colaboración

Versión: [2], data [Abril/2018]

Se deberán firmar dos modelos, uno será entregado al participante y otro será conservado por el responsable del estudio de investigación

DOCUMENTO DE CONSENTIMIENTO PARA LA PARTICIPACIÓN EN UN ESTUDIO DE INVESTIGACIÓN

TÍTULO del estudio: Análisis geométrico y hemodinámico del riesgo de ruptura en aneurismas intracraneales.

Yo,.....

- Leí la hoja de información al participante del estudio arriba mencionado que se me entregó, pude conversar con: y hacer todas las preguntas sobre el estudio.
- Comprendo que mi participación es voluntaria, y que puedo retirarme del estudio cuando quiera, sin tener que dar explicaciones y sin que esto repercuta en mis cuidados médicos.
- Accedo a que se utilicen mis datos en las condiciones detalladas en la hoja de información al participante.
- Presto libremente mi conformidad para participar en este estudio.

Fdo.: El/la participante,

Fdo.: El/la investigador/a que solicita el consentimiento

Nombre y Apellidos:

Nombre y Apellidos:

Fecha:

Fecha:

Versión: [2], data [Abril/2018]

Se deberán firmar dos modelos, uno será entregado al participante y otro será conservado por el responsable del estudio de investigación

DOCUMENTO DE CONSENTIMIENTO ANTE TESTIGOS PARA LA PARTICIPACIÓN EN UN ESTUDIO DE INVESTIGACIÓN (para los casos en que el participante no puede leer/escribir)

El testigo imparcial ha de identificarse e ser una persona ajena al equipo investigador.

TÍTULO del estudio: Análisis geométrico y hemodinámico del riesgo de ruptura en aneurismas intracraneales.

Yo,....., como testigo imparcial, afirmo que en mi presencia:

- Se le leyó a..... la hoja de información al participante del estudio arriba mencionado que se le entregó, y pudo hacer todas las preguntas sobre el estudio.
- Comprendió que su participación es voluntaria, y que puede retirarse del estudio cuando quiera, sin tener que dar explicaciones y sin que esto repercuta en sus cuidados médicos.
- Accede a que se utilicen sus datos en las condiciones detalladas en la hoja de información al participante.
- Presta libremente su conformidad para participar en este estudio.

Fdo.: El/la testigo,

Fdo.: El/la investigador/a que solicita el consentimiento

Nombre y apellidos:

Nombre y Apellidos:

Fecha:

Fecha:

Versión: [2], data [Abril/2018]

Se deberán firmar dos modelos, uno será entregado al participante y otro será conservado por el responsable del estudio de investigación

DOCUMENTO DE CONSENTIMIENTO PARA REPRESENTANTE LEGAL PARA LA PARTICIPACIÓN EN UN ESTUDIO DE INVESTIGACIÓN

TÍTULO del estudio: Análisis geométrico y hemodinámico del riesgo de ruptura en aneurismas intracraneales.

Yo, _____, representante legal de _____

- Leí la hoja de información al participante del estudio arriba mencionado que se me entregó, pude conversar con y hacer todas las preguntas sobre el estudio.
- Comprendo que su participación es voluntaria, y que pueden retirarse del estudio cuando quiera, sin tener que dar explicaciones y sin que esto repercuta en sus cuidados médicos.
- Acceso a que se utilicen sus datos en las condiciones detalladas en la hoja de información al participante.
- Presto libremente mi conformidad para que participe en este estudio.

Fdo.: El/la representante legal,

Fdo.: El/la investigador/a que solicita el consentimiento

Nombre e apellidos:

Nombre e apellidos:

Fecha:

Fecha:

Versión: [2], data [Abril/2018]

Se deberán firmar dos modelos, uno será entregado al participante y otro será conservado por el responsable del estudio de investigación



REFERENCES

1. Schievink WI. Intracranial aneurysms. *New Engl J Med*. 1997;336(1):28-40.
2. Rinkel GJ, Djibuti M, Algra A, van Gijn J. Prevalence and risk of rupture of intracranial aneurysms: a systematic review. *Stroke*. 1998;29(1):251-256.
3. Meng H, Tutino VM, Xiang J, Siddiqui A. High WSS or low WSS? Complex interactions of hemodynamics with intracranial aneurysm initiation, growth, and rupture: toward a unifying hypothesis. *AJNR Am J Neuroradiol*. 2014;35(7):1254-1262.
4. Toth G, Cerejo R. Intracranial aneurysms: Review of current science and management. *Vasc Med*. 2018;23(3):276-288.
5. Vlak MH, Algra A, Brandenburg R, Rinkel GJ. Prevalence of unruptured intracranial aneurysms, with emphasis on sex, age, comorbidity, country, and time period: a systematic review and meta-analysis. *Lancet Neurol*. 2011;10(7):626-636.
6. Vlak MH, Rinkel GJ, Greebe P, Algra A. Independent risk factors for intracranial aneurysms and their joint effect: a case-control study. *Stroke*. 2013;44(4):984-987.
7. van Gijn J, Rinkel GJE. Subarachnoid haemorrhage: diagnosis, causes and management. *Brain*. 2001;124(2):249-278.
8. Signorelli F, Gory B, Riva R, Labeyrie P-E, Pelissou-Guyotat I, Turjman F. Hemodynamics, inflammation, vascular remodeling, and the development and rupture of intracranial aneurysms: a review. *Neuroimmunology and Neuroinflammation*. 2015;2(2):59.
9. Chalouhi N, Hoh BL, Hasan D. Review of cerebral aneurysm formation, growth, and rupture. *Stroke*. 2013;44(12):3613-3622.
10. Ronkainen A, Puranen MI, Hernesniemi JA, et al. Intracranial aneurysms: MR angiographic screening in 400 asymptomatic individuals with increased familial risk. *Radiology*. 1995;195(1):35-40.
11. Raaymakers TW. Aneurysms in relatives of patients with subarachnoid hemorrhage: frequency and risk factors. MARS Study

- Group. Magnetic Resonance Angiography in Relatives of patients with Subarachnoid hemorrhage. *Neurology*. 1999;53(5):982-988.
12. Magnetic Resonance Angiography in Relatives of Patients with Subarachnoid Hemorrhage Study G. Risks and benefits of screening for intracranial aneurysms in first-degree relatives of patients with sporadic subarachnoid hemorrhage. *N Engl J Med*. 1999;341(18):1344-1350.
 13. de Rooij NK, Linn FHH, van der Plas JA, Algra A, Rinkel GJE. Incidence of subarachnoid haemorrhage: a systematic review with emphasis on region, age, gender and time trends. *Journal of Neurology, Neurosurgery & Psychiatry*. 2007;78(12):1365-1372.
 14. Suarez JL, Tarr RW, Selman WR. Aneurysmal subarachnoid hemorrhage. *New Eng J Med*. 2006;354(4):387-396.
 15. Nieuwkamp DJ, Setz LE, Algra A, Linn FHH, de Rooij NK, Rinkel GJE. Changes in case fatality of aneurysmal subarachnoid haemorrhage over time, according to age, sex, and region: a meta-analysis. *Lancet Neurol*. 2009;8(7):635-642.
 16. Etminan N, Chang H-S, Hackenberg K, et al. Worldwide Incidence of Aneurysmal Subarachnoid Hemorrhage According to Region, Time Period, Blood Pressure, and Smoking Prevalence in the Population: A Systematic Review and Meta-analysis. *JAMA neurology*. 2019.
 17. Sarti C, Tuomilehto J, Salomaa V, et al. Epidemiology of subarachnoid hemorrhage in Finland from 1983 to 1985. *Stroke*. 1991;22(7):848-853.
 18. Kozak N, Hayashi M. Trends in the incidence of subarachnoid hemorrhage in Akita Prefecture, Japan. *J Neurosurg*. 2007;106(2):234-238.
 19. Eden SV, Meurer WJ, Sanchez BN, et al. Gender and ethnic differences in subarachnoid hemorrhage. *Neurology*. 2008;71(10):731-735.
 20. Huang Y-H, Liao C-C, Yang K-Y. Demographics and short-term outcomes of spontaneous subarachnoid hemorrhage in young adults. *World Neurosurg*. 2017;102:414-419.
 21. Rutten-Jacobs LCA, Arntz RM, Maaijwee NAM, et al. Long-term mortality after stroke among adults aged 18 to 50 years. *Jama*. 2013;309(11):1136-1144.

22. Koivunen RJ, Tatlisumak T, Satopää J, Niemelä M, Putaala J. Intracerebral hemorrhage at young age: long - term prognosis. *European journal of neurology*. 2015;22(7):1029-1037.
23. Johnston SC, Selvin S, Gress DR. The burden, trends, and demographics of mortality from subarachnoid hemorrhage. *Neurology*. 1998;50(5):1413-1418.
24. Rivero-Arias O, Gray A, Wolstenholme J. Burden of disease and costs of aneurysmal subarachnoid haemorrhage (aSAH) in the United Kingdom. *Cost Effectiveness and Resource Allocation*. 2010;8(1):6.
25. Hütter BO, Gilsbach JM. Early neuropsychological sequelae of aneurysm surgery and subarachnoid haemorrhage. *Acta neurochirurgica*. 1996;138(12):1370-1379.
26. von Vogelsang AC, Wengström Y, Forsberg C. Patient information after ruptured intracranial aneurysm. *Journal of advanced nursing*. 2004;48(6):551-559.
27. Vilkki J, Holst P, Öhman J, Servo A, Heiskanen O. Social outcome related to cognitive performance and computed tomographic findings after surgery for a ruptured intracranial aneurysm. *Neurosurgery*. 1990;26(4):579-585.
28. Wiebers DO, Whisnant JP, Huston J, 3rd, et al. Unruptured intracranial aneurysms: natural history, clinical outcome, and risks of surgical and endovascular treatment. *Lancet*. 2003;362(9378):103-110.
29. Polmear A. Sentinel headaches in aneurysmal subarachnoid haemorrhage: what is the true incidence? A systematic review. *Cephalalgia*. 2003;23(10):935-941.
30. Sayer D, Bloom B, Fernando K, et al. An Observational Study of 2,248 Patients Presenting With Headache, Suggestive of Subarachnoid Hemorrhage, Who Received Lumbar Punctures Following Normal Computed Tomography of the Head. *Acad Emerg Med*. 2015;22(11):1267-1273.
31. van Gelder JM. Computed tomographic angiography for detecting cerebral aneurysms: implications of aneurysm size distribution for the sensitivity, specificity, and likelihood ratios. *Neurosurgery*. 2003;53(3):597-605; discussion 605-596.
32. Botterell EH, Loughheed WM, Scott JW, Vandewater SL. Hypothermia, and interruption of carotid, or carotid and vertebral circulation, in

- the surgical management of intracranial aneurysms. *Journal of neurosurgery*. 1956;13(1):1-42.
33. Hunt WE, Hess RM. Surgical risk as related to time of intervention in the repair of intracranial aneurysms. *J Neurosurg*. 1968;28(1):14-20.
 34. Teasdale GM, Drake CG, Hunt W, et al. A universal subarachnoid hemorrhage scale: report of a committee of the World Federation of Neurosurgical Societies. *Journal of neurology, neurosurgery, and psychiatry*. 1988;51(11):1457.
 35. Hirai S, Ono J, Yamaura A. Clinical grading and outcome after early surgery in aneurysmal subarachnoid hemorrhage. *Neurosurgery*. 1996;39(3):441-446.
 36. Ogilvy CS, Carter BS. A proposed comprehensive grading system to predict outcome for surgical management of intracranial aneurysms. *Neurosurgery*. 1998;42(5):959-968.
 37. Vega C, Kwoon JV, Lavine SD. Intracranial aneurysms: current evidence and clinical practice. *Am Fam Physician*. 2002;66(4):601-608.
 38. Brisman JL, Song JK, Newell DW. Cerebral aneurysms. *N Engl J Med*. 2006;355(9):928-939.
 39. Jakubowski J, Kendall B. Coincidental aneurysms with tumours of pituitary origin. *J Neurol Neurosurg Psychiatry*. 1978;41(11):972-979.
 40. Ajiboye N, Chalouhi N, Starke RM, Zanaty M, Bell R. Unruptured Cerebral Aneurysms: Evaluation and Management. *ScientificWorldJournal*. 2015;2015:954954.
 41. Nieuwkamp DJ, Setz LE, Algra A, Linn FH, de Rooij NK, Rinkel GJ. Changes in case fatality of aneurysmal subarachnoid haemorrhage over time, according to age, sex, and region: a meta-analysis. *Lancet Neurol*. 2009;8(7):635-642.
 42. Williams LN, Brown RD, Jr. Management of unruptured intracranial aneurysms. *Neurol Clin Pract*. 2013;3(2):99-108.
 43. Bonita R. Cigarette smoking, hypertension and the risk of subarachnoid hemorrhage: a population-based case-control study. *Stroke*. 1986;17(5):831-835.
 44. Investigators UJ, Morita A, Kirino T, et al. The natural course of unruptured cerebral aneurysms in a Japanese cohort. *N Engl J Med*. 2012;366(26):2474-2482.

45. Greving JP, Wermer MJ, Brown RD, Jr., et al. Development of the PHASES score for prediction of risk of rupture of intracranial aneurysms: a pooled analysis of six prospective cohort studies. *Lancet Neurol*. 2014;13(1):59-66.
46. Korja M, Lehto H, Juvela S. Lifelong rupture risk of intracranial aneurysms depends on risk factors: a prospective Finnish cohort study. *Stroke*. 2014;45(7):1958-1963.
47. Connolly ES, Jr., Rabinstein AA, Carhuapoma JR, et al. Guidelines for the management of aneurysmal subarachnoid hemorrhage: a guideline for healthcare professionals from the American Heart Association/American Stroke Association. *Stroke*. 2012;43(6):1711-1737.
48. Committee for Guidelines for Management of Aneurysmal Subarachnoid Hemorrhage JSoSfCS. Evidence-based guidelines for the management of aneurysmal subarachnoid hemorrhage. English Edition. *Neurol Med Chir (Tokyo)*. 2012;52(6):355-429.
49. Bederson JB, Connolly ES, Jr., Batjer HH, et al. Guidelines for the management of aneurysmal subarachnoid hemorrhage: a statement for healthcare professionals from a special writing group of the Stroke Council, American Heart Association. *Stroke*. 2009;40(3):994-1025.
50. Aoki T, Kataoka H, Morimoto M, Nozaki K, Hashimoto N. Macrophage-derived matrix metalloproteinase-2 and -9 promote the progression of cerebral aneurysms in rats. *Stroke*. 2007;38(1):162-169.
51. Hasan DM, Mahaney KB, Magnotta VA, et al. Macrophage imaging within human cerebral aneurysms wall using ferumoxytol-enhanced MRI: a pilot study. *Arteriosclerosis, thrombosis, and vascular biology*. 2012;32(4):1032-1038.
52. Stehbens WE. Pathology and pathogenesis of intracranial berry aneurysms. *Neurol Res*. 1990;12(1):29-34.
53. Inci S, Spetzler RF. Intracranial aneurysms and arterial hypertension: a review and hypothesis. *Surg Neurol*. 2000;53(6):530-540; discussion 540-532.
54. Finlay HM, Whittaker P, Canham PB. Collagen organization in the branching region of human brain arteries. *Stroke*. 1998;29(8):1595-1601.

55. Steiger HJ. Pathophysiology of development and rupture of cerebral aneurysms. *Acta Neurochir Suppl (Wien)*. 1990;48:1-57.
56. Juvela S. Natural history of unruptured intracranial aneurysms: risks for aneurysm formation, growth, and rupture. *Acta Neurochir Suppl*. 2002;82:27-30.
57. Marbacher S, Schlappi JA, Fung C, Husler J, Beck J, Raabe A. Do statins reduce the risk of aneurysm development? A case-control study. *J Neurosurg*. 2012;116(3):638-642.
58. Aoki T, Nishimura M, Kataoka H, et al. Role of angiotensin II type 1 receptor in cerebral aneurysm formation in rats. *Int J Mol Med*. 2009;24(3):353-359.
59. Krischek B, Kasuya H, Tajima A, et al. Network-based gene expression analysis of intracranial aneurysm tissue reveals role of antigen presenting cells. *Neuroscience*. 2008;154(4):1398-1407.
60. Aoki T, Kataoka H, Morimoto M, Nozaki K, Hashimoto N. Macrophage-derived matrix metalloproteinase-2 and-9 promote the progression of cerebral aneurysms in rats. *Stroke*. 2007;38(1):162-169.
61. Metaxa E, Tremmel M, Natarajan SK, et al. Characterization of critical hemodynamics contributing to aneurysmal remodeling at the basilar terminus in a rabbit model. *Stroke*. 2010;41(8):1774-1782.
62. Jayaraman T, Berenstein V, Li X, et al. Tumor necrosis factor α is a key modulator of inflammation in cerebral aneurysms. *Neurosurgery*. 2005;57(3):558-564.
63. Korja M, Silventoinen K, McCarron P, et al. Genetic epidemiology of spontaneous subarachnoid hemorrhage: Nordic Twin Study. *Stroke*. 2010;41(11):2458-2462.
64. Pera J, Korostynski M, Krzyszkowski T, et al. Gene expression profiles in human ruptured and unruptured intracranial aneurysms: what is the role of inflammation? *Stroke*. 2010;41(2):224-231.
65. Lell MM, Anders K, Uder M, et al. New techniques in CT angiography. *Radiographics*. 2006;26 Suppl 1:S45-62.
66. Kouskouras C, Charitanti A, Giavroglou C, et al. Intracranial aneurysms: evaluation using CTA and MRA. Correlation with DSA and intraoperative findings. *Neuroradiology*. 2004;46(10):842-850.

67. Kumar A, Kato Y, Motoharu H, et al. An update on three-dimensional ct angiography in aneurysms: a useful modality for a neurosurgeon. *Turk Neurosurg.* 2013;23(3):304-311.
68. Raghavan ML, Ma B, Harbaugh RE. Quantified aneurysm shape and rupture risk. *J Neurosurg.* 2005;102(2):355-362.
69. Ujiie H, Tamano Y, Sasaki K, Hori T. Is the aspect ratio a reliable index for predicting the rupture of a saccular aneurysm? *Neurosurgery.* 2001;48(3):495-502; discussion 502-493.
70. Ujiie H, Tachibana H, Hiramatsu O, et al. Effects of size and shape (aspect ratio) on the hemodynamics of saccular aneurysms: a possible index for surgical treatment of intracranial aneurysms. *Neurosurgery.* 1999;45(1):119-129; discussion 129-130.
71. Tateshima S, Chien A, Sayre J, Cebral J, Vinuela F. The effect of aneurysm geometry on the intra-aneurysmal flow condition. *Neuroradiology.* 2010;52(12):1135-1141.
72. Dhar S, Tremmel M, Mocco J, et al. Morphology parameters for intracranial aneurysm rupture risk assessment. *Neurosurgery.* 2008;63(2):185-196; discussion 196-187.
73. Tremmel M, Dhar S, Levy EI, Mocco J, Meng H. Influence of intracranial aneurysm-to-parent vessel size ratio on hemodynamics and implication for rupture: results from a virtual experimental study. *Neurosurgery.* 2009;64(4):622-630; discussion 630-621.
74. Lin N, Ho A, Gross BA, et al. Differences in simple morphological variables in ruptured and unruptured middle cerebral artery aneurysms. *J Neurosurg.* 2012;117(5):913-919.
75. Hoh BL, Siström CL, Firment CS, et al. Bottleneck factor and height-width ratio: association with ruptured aneurysms in patients with multiple cerebral aneurysms. *Neurosurgery.* 2007;61(4):716-722; discussion 722-713.
76. Hassan T, Timofeev EV, Saito T, et al. A proposed parent vessel geometry-based categorization of saccular intracranial aneurysms: computational flow dynamics analysis of the risk factors for lesion rupture. *J Neurosurg.* 2005;103(4):662-680.
77. Xiang J, Natarajan SK, Tremmel M, et al. Hemodynamic-morphologic discriminants for intracranial aneurysm rupture. *Stroke.* 2011;42(1):144-152.

78. Cebra J, Mut F, Sforza D, et al. Clinical Application of Image-Based CFD for Cerebral Aneurysms. *Int J Numer Method Biomed Eng.* 2011;27(7):977-992.
79. Fishman EK, Ney DR, Heath DG, Corl FM, Horton KM, Johnson PT. Volume rendering versus maximum intensity projection in CT angiography: what works best, when, and why. *Radiographics.* 2006;26(3):905-922.
80. Zhu C, Wang X, Eisenmenger L, et al. Surveillance of Unruptured Intracranial Saccular Aneurysms Using Noncontrast 3D-Black-Blood MRI: Comparison of 3D-TOF and Contrast-Enhanced MRA with 3D-DSA. *AJNR Am J Neuroradiol.* 2019;40(6):960-966.
81. Khandelwal N, Gupta AK, Garg A. *Diagnostic Radiology: Neuroradiology including Head and Neck Imaging.* Jaypee Brothers, Medical Publishers Pvt. Limited; 2018.
82. Geers AJ, Larrabide I, Morales HG, Frangi AF. Comparison of steady-state and transient blood flow simulations of intracranial aneurysms. *Conf Proc IEEE Eng Med Biol Soc.* 2010;2010:2622-2625.
83. Shibeshi SS, Collins WE. The Rheology of Blood Flow in a Branched Arterial System. *Appl Rheol.* 2005;15(6):398-405.
84. Bergel DH. The static elastic properties of the arterial wall. *J Physiol.* 1961;156(3):445-457.
85. Zhang B, Gu J, Qian M, Niu L, Ghista D. Study of correlation between wall shear stress and elasticity in atherosclerotic carotid arteries. *Biomedical engineering online.* 2018;17(1):5-5.
86. Dempere-Marco L, Oubel E, Castro M, Putman C, Frangi A, Cebra J. CFD analysis incorporating the influence of wall motion: application to intracranial aneurysms. *Med Image Comput Comput Assist Interv.* 2006;9(Pt 2):438-445.
87. Xu L, Sugawara M, Tanaka G, Ohta M, Liu H, Yamaguchi R. Effect of elasticity on wall shear stress inside cerebral aneurysm at anterior cerebral artery. *Technol Health Care.* 2016;24(3):349-357.
88. Valencia A, Burdiles P, Ignat M, et al. Fluid structural analysis of human cerebral aneurysm using their own wall mechanical properties. *Comput Math Methods Med.* 2013;2013:293128.
89. Campbell IC, Ries J, Dhawan SS, Quyyumi AA, Taylor WR, Oshinski JN. Effect of inlet velocity profiles on patient-specific computational

- fluid dynamics simulations of the carotid bifurcation. *J Biomech Eng.* 2012;134(5):051001.
90. Blanco PJ, Muller LO, Spence JD. Blood pressure gradients in cerebral arteries: a clue to pathogenesis of cerebral small vessel disease. *Stroke Vasc Neurol.* 2017;2(3):108-117.
 91. Fedorov A, Beichel R, Kalpathy-Cramer J, et al. 3D Slicer as an image computing platform for the Quantitative Imaging Network. *Magn Reson Imaging.* 2012;30(9):1323-1341.
 92. Ahmed, Sutalo, Kavnoudias H, Madan A. Numerical investigation of hemodynamics of lateral cerebral aneurysm following coil embolization. *Engineering Applications of Computational Fluid Mechanics.* 2011;5:319-340.
 93. Bai-Nan X, Fu-Yu W, Lei L, Xiao-Jun Z, Hai-Yue J. Hemodynamics model of fluid-solid interaction in internal carotid artery aneurysms. *Neurosurg Rev.* 2011;34(1):39-47.
 94. Sforza DM, Kono K, Tateshima S, Vinuela F, Putman C, Cebal JR. Hemodynamics in growing and stable cerebral aneurysms. *J Neurointerv Surg.* 2016;8(4):407-412.
 95. Arzani A, Shadden SC. Characterizations and Correlations of Wall Shear Stress in Aneurysmal Flow. *J Biomech Eng.* 2016;138(1).
 96. Jou LD, Lee DH, Morsi H, Mawad ME. Wall shear stress on ruptured and unruptured intracranial aneurysms at the internal carotid artery. *AJNR Am J Neuroradiol.* 2008;29(9):1761-1767.
 97. Qiu T, Jin G, Xing H, Lu H. Association between hemodynamics, morphology, and rupture risk of intracranial aneurysms: a computational fluid modeling study. *Neurol Sci.* 2017;38(6):1009-1018.
 98. Metaxa E, Tremmel M, Natarajan SK, et al. Characterization of critical hemodynamics contributing to aneurysmal remodeling at the basilar terminus in a rabbit model. *Stroke.* 2010;41(8):1774-1782.
 99. Kolega J, Gao L, Mandelbaum M, et al. Cellular and molecular responses of the basilar terminus to hemodynamics during intracranial aneurysm initiation in a rabbit model. *J Vasc Res.* 2011;48(5):429-442.
 100. Meng H, Wang Z, Hoi Y, et al. Complex hemodynamics at the apex of an arterial bifurcation induces vascular remodeling resembling cerebral aneurysm initiation. *Stroke.* 2007;38(6):1924-1931.

101. Xiang J, Tutino VM, Snyder KV, Meng H. CFD: computational fluid dynamics or confounding factor dissemination? The role of hemodynamics in intracranial aneurysm rupture risk assessment. *AJNR Am J Neuroradiol*. 2014;35(10):1849-1857.
102. Juvela S, Porras M, Poussa K. Natural history of unruptured intracranial aneurysms: probability of and risk factors for aneurysm rupture. *J Neurosurg*. 2008;108(5):1052-1060.
103. Seshaiyer P, Hsu F, Shah A, Kyriacou S, HUMPHREY* J. Multiaxial mechanical behavior of human saccular aneurysms. *Computer Methods in Biomechanics and Biomedical Engineering*. 2001;4(3):281-289.
104. Polzer S, Gasser TC. Biomechanical rupture risk assessment of abdominal aortic aneurysms based on a novel probabilistic rupture risk index. *J R Soc Interface*. 2015;12(113):20150852.
105. Kaminogo M, Yonekura M, Shibata S. Incidence and outcome of multiple intracranial aneurysms in a defined population. *Stroke*. 2003;34(1):16-21.
106. Shen X, Xu T, Ding X, Wang W, Liu Z, Qin H. Multiple intracranial aneurysms: endovascular treatment and complications. *Interv Neuroradiol*. 2014;20(4):442-447.
107. Cho WS, Kim JE, Park SQ, et al. Korean Clinical Practice Guidelines for Aneurysmal Subarachnoid Hemorrhage. *J Korean Neurosurg Soc*. 2018;61(2):127-166.
108. Berg P, Janiga G, Beuing O, Neugebauer M, Thévenin D. Hemodynamics in Multiple Intracranial Aneurysms: The Role of Shear Related to Rupture.
109. Jou L, Britz G. Correlation Between Aneurysm Size and Hemodynamics in One Individual with Multiple Small Intracranial Aneurysms. *Cureus*. 2016;8(7):e683.
110. Jing L, Liu J, Zhang Y, et al. Analysis of Multiple Intracranial Aneurysms with Different Outcomes in the Same Patient After Endovascular Treatment. *World Neurosurg*. 2016;91:399-408.
111. Castro MA, Putman CM, Cebal JR. Computational fluid dynamics modeling of intracranial aneurysms: effects of parent artery segmentation on intra-aneurysmal hemodynamics. *AJNR Am J Neuroradiol*. 2006;27(8):1703-1709.

112. Zanaty M, Chalouhi N, Tjoumakaris SI, Fernando Gonzalez L, Rosenwasser RH, Jabbour PM. Aneurysm geometry in predicting the risk of rupture. A review of the literature. *Neurol Res.* 2014;36(4):308-313.
113. Andic C, Aydemir F, Kardes O, Gedikoglu M, Akin S. Single-stage endovascular treatment of multiple intracranial aneurysms with combined endovascular techniques: is it safe to treat all at once? *J Neurointerv Surg.* 2017;9(11):1069-1074.
114. Vrselja Z, Brkic H, Mrdenovic S, Radic R, Curic G. Function of circle of Willis. *J Cereb Blood Flow Metab.* 2014;34(4):578-584.
115. Jabbarli R, Reinhard M, Roelz R, et al. Clinical relevance of anterior cerebral artery asymmetry in aneurysmal subarachnoid hemorrhage. *J Neurosurg.* 2017;127(5):1070-1076.
116. Rinaldo L, McCutcheon BA, Murphy ME, Bydon M, Rabinstein AA, Lanzino G. Relationship of A1 segment hypoplasia to anterior communicating artery aneurysm morphology and risk factors for aneurysm formation. *J Neurosurg.* 2017;127(1):89-95.
117. Kaspera W, Ladzinski P, Larysz P, et al. Morphological, hemodynamic, and clinical independent risk factors for anterior communicating artery aneurysms. *Stroke.* 2014;45(10):2906-2911.
118. Zhang XJ, Gao BL, Hao WL, Wu SS, Zhang DH. Presence of Anterior Communicating Artery Aneurysm Is Associated With Age, Bifurcation Angle, and Vessel Diameter. *Stroke.* 2018;49(2):341-347.
119. Lin N, Ho A, Charoenvimolphan N, Frerichs KU, Day AL, Du R. Analysis of morphological parameters to differentiate rupture status in anterior communicating artery aneurysms. *PLoS One.* 2013;8(11):e79635.
120. Cai W, Shi D, Gong J, et al. Are Morphologic Parameters Actually Correlated with the Rupture Status of Anterior Communicating Artery Aneurysms? *World Neurosurg.* 2015;84(5):1278-1283.
121. Maiti TK, Bir SC, Patra DP, Cuellar H, Nanda A. 158 Morphological Parameters for Anterior Communicating Artery Aneurysm Rupture Risk Assessment. *Neurosurgery.* 2016;63(CN_suppl_1):163-164.
122. Zhou G, Zhu Y, Yin Y, Su M, Li M. Association of wall shear stress with intracranial aneurysm rupture: systematic review and meta-analysis. *Sci Rep.* 2017;7(1):5331.

123. Lee CJ, Zhang Y, Takao H, Murayama Y, Qian Y. The influence of elastic upstream artery length on fluid-structure interaction modeling: a comparative study using patient-specific cerebral aneurysm. *Med Eng Phys.* 2013;35(9):1377-1384.
124. Humphrey J, Canham P. Structure, mechanical properties, and mechanics of intracranial saccular aneurysms. *Journal of elasticity and the physical science of solids.* 2000;61(1-3):49-81.
125. Valencia A, Torres F. Effects of hypertension and pressure gradient in a human cerebral aneurysm using fluid structure interaction simulations. *Journal of Mechanics in Medicine and Biology.* 2017;17(01):1750018.
126. MacDonald DJ, Finlay HM, Canham PB. Directional wall strength in saccular brain aneurysms from polarized light microscopy. *Ann Biomed Eng.* 2000;28(5):533-542.
127. Frosen J, Tulamo R, Paetau A, et al. Saccular intracranial aneurysm: pathology and mechanisms. *Acta Neuropathol.* 2012;123(6):773-786.
128. Suzuki T, Stapleton CJ, Koch MJ, et al. Decreased wall shear stress at high-pressure areas predicts the rupture point in ruptured intracranial aneurysms. *J Neurosurg.* 2019:1-7.
129. Voß S, Saalfeld S, Hoffmann T, et al. Fluid-Structure Simulations of a Ruptured Intracranial Aneurysm: Constant versus Patient-Specific Wall Thickness. *Computational and Mathematical Methods in Medicine.* 2016;2016:1-8.
130. Nornes H. The role of intracranial pressure in the arrest of hemorrhage in patients with ruptured intracranial aneurysm. *J Neurosurg.* 1973;39(2):226-234.
131. Thenier-Villa JL, Riveiro Rodríguez A, González-Vargas PM, Martínez-Rolán RM, Gelabert-González M, Badaoui Fernández A, et al: Effects of external ventricular drainage decompression of intracranial hypertension on rebleeding of brain aneurysms: A fluid structure interaction study. *Interdisciplinary Neurosurgery.* 2020;19:100613
132. Thenier-Villa JL, Riveiro Rodriguez A, Martinez-Rolan RM, Gelabert-Gonzalez M, Gonzalez-Vargas PM, Calero-Felix L, et al: A1 asynchrony, a potential risk factor for the rupture of anterior communicating artery aneurysms: A computational fluid dynamics study. *Neurocirugia (Astur).* 2020;30:207-214

133. Thenier-Villa JL, Riveiro Rodriguez A, Martinez-Rolan RM, Gelabert-Gonzalez M, Gonzalez-Vargas PM, Galarraga Campoverde RA, et al: Hemodynamic Changes in the Treatment of Multiple Intracranial Aneurysms: A Computational Fluid Dynamics Study. *World Neurosurg.* 2018;118:e631-e638

